Physics – Uspekhi **50** (2) 197 – 218 (2007)

REVIEWS OF TOPICAL PROBLEMS PACS numbers: **73.43.–f**, 73.43.Fj

Edge states in the regimes of integer and fractional quantum Hall effects

E V Deviatov

DOI: 10.1070/PU2007v050n02ABEH006244

Contents

Abstract. The current state of research into the structure and properties of edge states emerging in the regimes of integer and fractional quantum Hall effect is reviewed. A consistent description of the results obtained for these two regimes allows specifying the effects caused by the electron – electron interaction. The most important areas of further studies are outlined.

1. Introduction

Surface states in quantizing magnetic fields have been known since the 1960s from the works by Khaikin on three-dimensional metals [1]. From the standpoint of semiclassical theory, these states arise as 'electron orbital jumps' near the boundary of a sample in a quantizing magnetic field whenever the cyclotron radius of an electron becomes smaller than the sample thickness. It is easy to see that the dimensionality of surface states is less than that of a bulk system by unity. For a three-dimensional metal, the surface states are quasi-two-dimensional.

In the 1970s, due to the progress in technology, it became possible to manufacture high-mobility two-dimensional systems. For a two-dimensional system, surface states in a quantizing magnetic field are already quasi-one-dimensional and should more accurately be termed edge states.

Of particular interest is the study of edge-state transport in the regime of the quantum Hall effect, where the Fermi level of the bulk sample lies within the mobility gap and the edge-state transport has a substantial influence on the properties of the system. Both the integer quantum Hall effect (IQHE) and the fractional quantum Hall effect (FQHE) occur in high-mobility two-dimensional electron systems in a quantizing magnetic field under low temperatures, of the order of the temperature of liquid helium (see Ref. [2] for a good, although outdated review). Both effects manifest themselves as plateaus in the Hall resistance $R_{xy} = (h/e^2)1/\nu$, where the filling factor ν is, correspondingly, an integer $1, 2, \ldots$ or a ratio of a particular form, $1/3, 2/3, 2/5, 3/5, \ldots$. The dissipative component of the magnetoresistance tensor R_{xx} then vanishes. Although the Fermi level is within the spectrum gap in both regimes, the origins of the gap are substantially different for the IQHE and FQHE. The integer quantum Hall effect is explained by the Landau quantization in the spectrum of the two-dimensional electron system in a magnetic field, and the electron – electron interaction is not relevant for it. On the contrary, the FQHE is fully recognized as a manifestation of the electron – electron interaction.

Even in the IQHE regime, where the electron – electron interaction can be neglected, one-dimensional edge states exhibit a plethora of interesting physical effects. The general approach to their description consists in the application of the Landauer formalism of one-dimensional channels [3], which was adopted by Büttiker for the analysis of edge states in two-dimensional systems [4]. Consistently taking the electron – electron interaction into account, which is necessary in the FQHE case, allows expecting that one-dimensional edge states exhibit effects typical of a one-dimensional electron liquid. We note that edge states in the FQHE regime are the only systems where the Luttinger model [5] of one-dimensional liquid is *exactly* valid and where each assumption of this model acquires a clear physical meaning, as was shown theoretically by Wen [6].

E V Deviatov Institute of Solid State Physics,
Russian Academy of Sciences,
142432 Chernogolovka, Moscow Region, Russian Federation
Tel. (7-495) 993 47 47 22946. Fax (7-496) 524 97 01
E-mail: dev@issp.ac.ru

Received 3 October 2006
Uspekhi Fizicheskikh Nauk **177** (2) 207 – 229 (2007)
Translated by M V Chekhova; edited by A M Semikhatov

In this review, the IQHE and FQHE regimes for edge states are considered separately in Sections 2 and 3, respectively. This allows us to first concentrate on the description of single-particle effects in the IQHE regime and then pass to the effects caused by inter-electron interaction (the FQHE regime).

During the nearly twenty years of research on edge states in the quantum Hall effect regime, no reviews have been published in Russian. The existing works in English are quite out of date [7], while the number of original papers, only in the journals of the American Physical Society, by far exceeds a thousand. It is therefore hopeless to present a 'historical' narrative focused on the sequence in which results were obtained or ideas were developed. This review only describes the main areas of study and the most well-established results, together with their critical analysis. In the Conclusion, the most significant fields of further development are formulated.

2. Edge states in the integer quantum Hall effect

2.1 Integer quantum Hall effect

As mentioned in the Introduction, the integer quantum Hall effect manifests itself in the Hall resistance taking values that are integer multiples of h/e^2, while the diagonal (dissipative) component of the resistance tensor tends to zero. This behavior of the resistance can be explained by the existence of gaps in the spectrum of a two-dimensional electron system in a quantizing magnetic field. The problem of calculating the spectrum of noninteracting electrons in a quantizing magnetic field was first solved by Landau [8]. Although the solution is widely known, we recall it here because we need it in what follows. Other important points in the theory of the IQHE, such as the reservoir theory, the roles of disorder and percolation, and screening, either are insignificant for the description of the edge states, and are therefore ignored here, or are introduced in the course of our consideration.

2.1.1 The spectrum of noninteracting electrons in a magnetic field. We find the energy levels of a free electron in a constant homogeneous magnetic field [8]. The vector potential is chosen in the Landau gauge, $\mathbf{A} = (-Hy, 0, 0)$ (the H field is directed along the z axis). The Hamiltonian is written as

$$H = \frac{1}{2m}\left(p_x + \frac{eH}{c}\,y\right)^2 + \frac{p_y^2}{2m}\,, \tag{1}$$

where, for simplicity, we ignore the spin and assume two-dimensional motion in the xy plane. The solution of the Schrödinger equation $H\psi = E\psi$ is sought in the form

$$\psi = \exp\left(\frac{\mathrm{i}}{\hbar}\,p_x x\right)\chi(y)\,, \tag{2}$$

which leads to the well-known harmonic oscillator equation,

$$\chi'' + \frac{2m}{\hbar^2}\left[E - \frac{m}{2}\left(\frac{eH}{mc}\right)^2 (y - y_0)^2\right]\chi = 0\,, \tag{3}$$

where $y_0 = -cp_x/(eH) = -l_{\mathrm{H}}^2 k_x$ is the so-called guiding center coordinate and $l_{\mathrm{H}} = [c\hbar/(eH)]^{1/2}$ is the magnetic length. Equation (3) yields the energy levels of the electron in a magnetic field,

$$E = \frac{|e|H}{mc}\,\hbar\left(n + \frac{1}{2}\right)\,, \tag{4}$$

where m is the band mass, e is the electron charge, and $n = 0, 1, 2, \ldots$ is the quantum level number. In other words, the problem of describing an electron in a magnetic field is reduced to the problem of finding dimensional quantization levels in a parabolic potential. The energy levels are equidistant and separated from each other by the cyclotron gap $\hbar\omega_{\mathrm{c}}$. This kind of quantization is called the Landau quantization, and the corresponding energy levels are called the Landau levels.

The existence of electron spin leads to an additional spin splitting of the Landau levels (the Zeeman splitting), while the existence of isospin in double-layer systems leads to isospin (symmetric – antisymmetric) splitting. The existence of gaps in the spectrum of the electron system is responsible for the IQHE regime.

The choice of the x, y axes is arbitrary so far (while the sample is considered infinite). Moreover, the obtained solution is obviously independent of the gauge. (The problem could be solved in the centrally symmetric gauge, where electron motion could be decomposed into the azimuthal one, described by a wave function of the form $\exp(\mathrm{i}\theta m)$, with θ being the azimuthal angle, and the radial one, given by the same Schrödinger equation (3) for the harmonic oscillator.)

2.1.2. Introducing the sample boundary into the problem. In the presence of a boundary, the geometry of the problem already suggests a preferred direction, the one along the edge. A reasonable choice of the gauge implies that the separation of variables in (2) is maintained and the edge potential only enters Eqn (3). With the help of a corresponding gauge, this can be done for any geometry of the sample — for instance, for a strip bounded from both sides (the Hall bar) or for a disc (Corbino).

Thus, Eqn (3) describes the motion of an electron in a parabolic potential, which increases to the first quantized value $\hbar\omega_{\mathrm{c}}/2$ over the distance equal to the magnetic length $l_{\mathrm{H}} = (c\hbar/eH)^{1/2}$. In the presence of the sample boundary, a term of the form $U(y)$ must be introduced into Eqn (3). Two limit cases are possible here:

(1) as y varies by a distance equal to the magnetic length l_{H}, the variation of the edge potential $U(y)$ is much larger than or comparable to the cyclotron energy $\hbar\omega_{\mathrm{c}}$;

(2) as y varies by a distance equal to the magnetic length l_{H}, the variation of the edge potential $U(y)$ is much smaller than the cyclotron energy $\hbar\omega_{\mathrm{c}}$.

In the first case, the potential is sharp, and the energy levels near the edge are found by solving the Schrödinger equation with a real profile $U(y)$, which leads to the spreading of energy levels in the vicinity of the boundary and to a considerable increase in the inter-level distance. (The last fact can be understood from the symmetry of the wave function.) In the second case, the edge potential makes the bottom of the subband increase smoothly near the edge, with the distance between the levels remaining almost constant.

2.2 Introducing edge states and the transport along the sample edge

As we show in Section 2.3.3, edge-state transport along the edge of the sample can be studied regardless of the actual structure of the edge. In this section, we therefore dwell on the ideas developed for the simplest case where the potential wall is infinitely high.

2.2.1 Halperin's idea. Halperin [9] was the first to consider an infinitely high potential wall bounding the sample in the regime of the quantum Hall effect (Fig. 1). He introduced current-carrying edge states as the intersections of the Landau levels and the Fermi level near the sample edges. Hence, the total number of edge states is equal to the filling factor, i.e., the number of filled Landau levels, and their electrochemical potentials are equal to the electrochemical potentials of the corresponding edges of the sample. We calculate the current along the sample. The density of the current at a Landau level is $j = n_{\mathrm{L}} e v$, where $n_{\mathrm{L}} = 1/2\pi l_{\mathrm{H}}^2$ is the density of states on the Landau level, e is the electron charge, and $v = (\partial E/\partial k)/\hbar$. Then the total current can be written as

$$I = \int_{y_1}^{y_2} j\,\mathrm{d}y = -\int_{k_1}^{k_2} j\, l_{\mathrm{H}}^2\,\mathrm{d}k$$
$$= \frac{e}{h}\int_{k_1}^{k_2} \frac{\partial E}{\partial k}\,\mathrm{d}k = \frac{e}{h}\int_{\mu_1}^{\mu_2} \mathrm{d}E = \frac{e}{h}(\mu_1 - \mu_2)\,. \qquad (5)$$

If the number of filled Landau levels is n, the total current through the sample can be written as $I = n(e/h)\Delta\mu$, where $\Delta\mu$ is the difference in the electrochemical potentials of the sample edges. Hence, the current is determined only by the difference in electrochemical potentials of the edges (or, in other words, of the edge states) and the number of filled Landau levels (the number of edge states). If we introduce the edge-state current $(e/h)\,\mu$, then the sum of all edge-state currents gives the total current through the sample.

The main goal of Halperin's work was to explain the quantization of the Hall resistance. Edge states were introduced for a perfect system (in the absence of disorder) and their role in the analysis was auxiliary.

2.2.2 The Büttiker – Landauer formalism. Büttiker [4] combined Halperin's idea of current-carrying edge states with the Landauer formalism, aiming to take scattering in one-dimensional semiconductors into account. He showed that the effects of elastic and nonelastic scattering in edge states and contacts can be taken into account by introducing the transmission coefficient matrix T_{ij}. He suggested the formalism for calculating various resistances for samples with many ohmic contacts (Fig. 2). In this formalism, the current I_i carried by edge states from a contact i is given by

$$I_i = \frac{e}{h}\left(n_i\mu_i + \sum_{j\neq i} T_{ij}\mu_j\right), \qquad (6)$$

where μ_i is the electrochemical potential of the contact i and n_i is the number of edge states coming from the contact i. It is easy to see that in the simplest case of a sample with two ideal contacts and in the absence of scattering, the total current through the contacts is given by the same relation (5) that was first obtained by Halperin.

Originally, Büttiker planned to use this formalism to explain the accuracy of the Hall resistance quantization in 'open' samples connected with reservoirs (ohmic contacts). But this formalism is much more powerful; it provides a method of calculating transport characteristics in samples having multiple contacts with different, in the general case, electrochemical potentials.

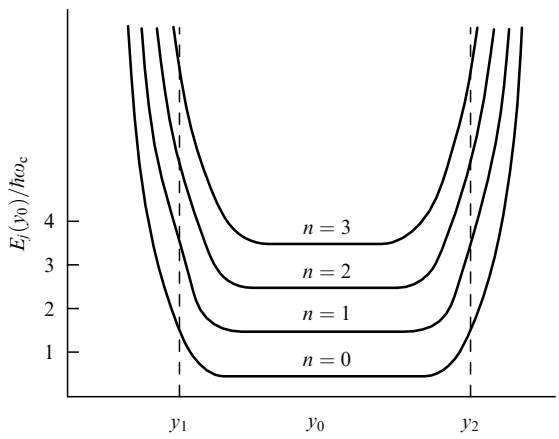

Figure 1. Behavior of the Landau levels near the sample edges in the case of an infinitely high potential wall. (From Ref. [4].)

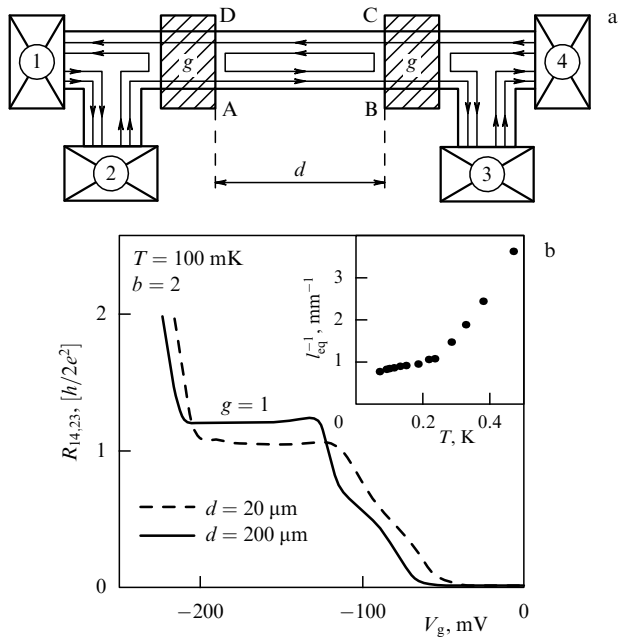

Figure 2. (a) Geometry of the Hall bar with two crossing gates. Crossed and numbered rectangles denote ohmic contacts. Shaded areas are gates coated onto the sample. The structure of edge states is shown for the filling factors $g = 1$ beneath the gate and $b = 2$ in the rest of the sample. (b) Deviation of the measured resistance as a measure of equilibration between the edge states. The inset shows the temperature dependence of the equilibration length for spin-split edge states. The dependence gives an idea of the scales of the values. (From Ref. [10].)

2.2.3 Experimental verification. Experimental testing of Buttiker's formalism was performed mainly in the Hall-bar geometry with crossing gates (see Fig. 2). In this geometry, a sample with two current and several potential contacts was crossed by one or several gates. With the current between the source-drain contacts (1 – 4 in Fig. 2) fixed, the voltage drop between the potential contacts (2 – 3 in Fig. 2) was measured. For a sample under the quantum Hall effect with the filling factor equal to two, the voltage drop is equal to zero. Reducing the electron concentration beneath one of the gates (with the second gate disregarded for simplicity) to the smaller filling factor equal to unity results in a nonzero voltage between contacts 2 and 3 corresponding to the resistance $R_{14,23} = (1/2)h/e^2$. This behavior can be easily

explained in terms of edge states: in the absence of voltage on the gate, two edge states leave contact 2 and the same states arrive at contact 3. Because no current flows through the potential contacts, their electrochemical potentials are equal, and the voltage U_{23} is therefore equal to zero at any current. If the filling factor beneath the gate is equal to 1, then one of the edge channels is reflected at the gate boundary while the other channel passes through, which leads to a more complicated set of electrochemical potentials of the contacts.

We give an example of a calculation in the Büttiker formalism (6) for this simple situation (we need such a calculation in what follows):

$$\begin{aligned} I_{14} &= (\mu_4 + \mu_2) - 2\mu_1 \text{ for contact 1}\,, \\ 0 &= 2\mu_1 - 2\mu_2 \text{ for contact 2}\,, \\ 0 &= \mu_2 + \mu_4 - 2\mu_3 \text{ for contact 3}\,, \\ -I_{14} &= 2\mu_4 - 2\mu_3 \text{ for contact 4}\,. \end{aligned} \tag{7}$$

The right-hand side of each equation in (7) contains the difference in the currents coming into and out of the corresponding contact, while the left-hand side contains the current through the contact (equal to zero for potential contacts and to the current through the sample for current contacts). For simplicity, the right-hand sides are written in $[e/h]$ units. The sought potential difference can be written as $U_{23} = (\mu_3 - \mu_2)/e$. By solving system (7), we obtain $I_{14} = 2(e^2/h)U_{23}$, which corresponds to the above value of the resistance $R_{14,23}$. We note that in obtaining this result, we used a collection of zeros and units as the matrix of transmission coefficients in Eqn (6) because some edge states completely pass beneath the gate, while others, on the contrary, are completely reflected.

Using this geometry, various effects considered by Büttiker have been simulated and studied (see Ref. [7] for a review of experiments on checking the Büttiker formalism). For instance, the nonideality of a contact means that edge states leave it with different electrochemical potentials. This behavior can be simulated by placing a crossing gate across the bar leading to the nonideal contact. As the filling factor beneath the gate decreases, one of the edge states is reflected at the input of the gate, similarly to the situation shown in Fig. 2, and this contact looks like a nonideal one for the rest of the sample, the degree of 'nonideality' being controllable by this gate. The contact can then be completely disconnected.

2.2.4 Transport across the edge. The case of small imbalance. In the domain between the gates (see Fig. 2), one of the edge channels starts from beneath the gate and the other approaches the gate along the gate edge. Their electrochemical potentials are different in general. Further along the sample edge, the electrochemical potentials of these channels come to an equilibrium due to the electron transport between them, i.e., across the sample edge. Thus, the transport effects between the edge states can be studied if the mixing of channels in the contact can be excluded, i.e., if a second crossing gate is used as a detector of the final electrochemical potential of the edge state, as shown in Fig. 2.

Using the Büttiker formalism in (6), it is easy to see that if equilibration of the electrochemical potentials of the edge states occurs in the region between the gates, the measured resistance is

$$R_{14,23} = \frac{h}{e^2}\left[1 + \exp\left(-\frac{2d}{l_{\mathrm{eq}}}\right)\right]^{-1}, \tag{8}$$

where l_{eq} is the phenomenological equilibration length between the edge states. Formula (8) has correct asymptotic behaviors: if the gates are close to each other ($d \ll l_{\mathrm{eq}}$), the second term in the square brackets tends to unity, as indeed should be the case for a single continuous gate; for gates placed far from each other ($d \gg l_{\mathrm{eq}}$), the second term is negligibly small, which corresponds to complete equilibration of the electrochemical potentials. The equilibration length l_{eq} can therefore be found from the deviation in the measured resistance from $h/2e^2$ (see Fig. 2).

Experimental data obtained by various groups (see, e.g., Ref. [10]) have shown that the equilibration length between spin-split edge states can reach 1 mm at low temperatures (the temperature of liquid helium) and is of the order of 100 μm for channels separated by a cyclotron gap. This difference is caused by the fact that the spin flip accompanying the electron transfer is hampered at the edge of the sample: there are no magnetic impurities in perfect heterostructures, and the spin flip is due to the spin – orbital and hyperfine interactions [11 – 13].

We note that such experiments provide information about the equilibration processes only for a small imbalance (a small difference in electrochemical potentials) between the edge states. This follows directly from Eqn (8), where at $d \ll l_{\mathrm{eq}}$ (the case of strongly nonequilibrium edge channels along the whole interaction length), the second term in the square brackets is exponentially small compared to the first one, which hinders accurate measurements [10]. But in the $d \gg l_{\mathrm{eq}}$ regime, the equilibration length is completely determined by the processes at small imbalance: even if the initial imbalance is large, it is reduced later due to equilibration of the edge states; the value of the equilibration length then depends on the final equilibration processes, which occur when the imbalance is small. This is the key feature for the geometry of the Hall bar with crossing gates, in which the transport between the edge states is considered a small correction to the transport along the edge.

Up to this point, the real structure of the edge has not been important for finding the phenomenological equilibration length. Before describing the special features of the transport between the edge states in the case of an arbitrary imbalance, where the details of the edge structure manifest themselves, we give a detailed description of the structure of a real (in most cases, etched or electrostatic) edge of a sample in Section 2.3.

2.3 Edge structure in real samples

2.3.1 Edge structure for an electrostatic edge potential. The question about the edge structure in the case of a model edge potential was most successfully considered in the works by Chklovskii, Shklovskii, and Glazman [14]. In the case of a smooth (electrostatic) potential, the bottom of the two-dimensional subband increases in approaching the edge of the sample, and the Landau levels follow the subband bottom (Fig. 3a). At any point, a local filling factor (the number of filled levels) can be introduced, which changes with a unit step from its initial value in the bulk of the sample to zero at the edge. A change in the local filling factor occurs each time a Landau level crosses the Fermi level. The authors of Ref. [14] took the electron – electron interaction into account in the mean-field approximation. It turned out that one-dimensional intersections of the Fermi and Landau levels are transformed into finite-width strips (in a certain region, the Landau level is 'pinned' to the Fermi level, see Fig. 3b) where

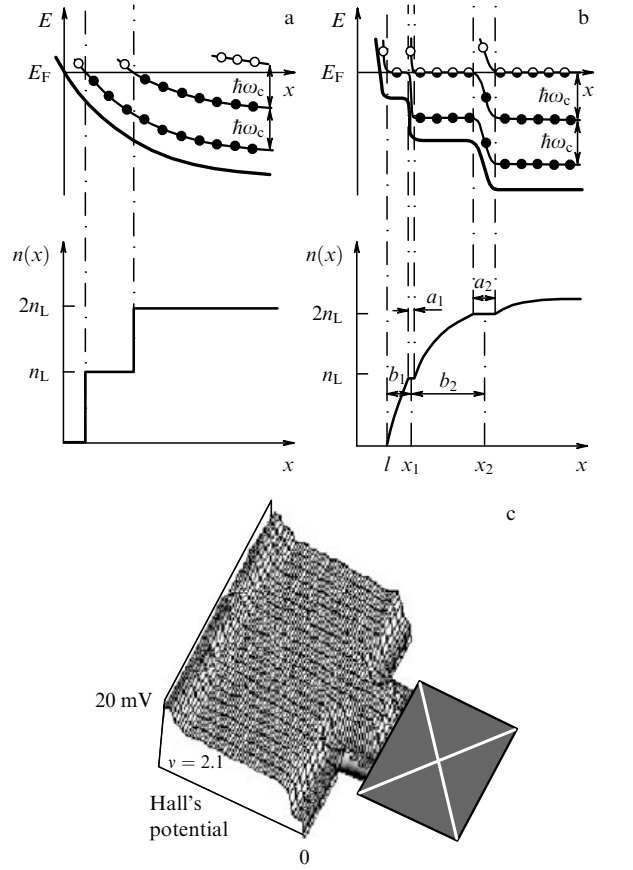

Figure 3. The structure of an edge in the case of a smooth potential (from Ref. [14]): (a) with the electron–electron interaction neglected; (b) reconstruction of the edge caused by the interaction; (c) visualization of the structure of a real sample (from Ref. [15]).

the local filling factor gradually varies, and the edge of the electron system is an alternating sequence of compressible and incompressible strips of electronic liquid. The strip width is determined by the energy gap between the corresponding Landau levels.

2.3.2 Edge structure for a real edge potential. The edge structure considered in Section 2.3.1 is closest to the experimental situation observed for etched and electrostatic edges in the IQHE regime. This is because a real edge potential is smooth. Indeed, because of the large absolute value of the cyclotron energy in the fields where the IQHE is observed, the edge potential always increases by a value much smaller than the cyclotron energy over the distance equal to the magnetic length. The strips of compressible and incompressible electron liquid can be observed directly in visualization experiments. For instance, the authors of Ref. [15] measured the capacitance between the tip of an atomic-force microscope and a two-dimensional electron gas (2DEG). The result, clearly demonstrating the existence of compressible and incompressible strips on the edge, is shown in Fig. 3c.

2.3.3 Distribution of the current over the sample. Considerations by Thouless. If the edge of the sample consists of alternating compressible and incompressible strips, the same questions arise: where does the current flow and why does the Büttiker formalism, which is based on a completely different picture, work so well? These questions were answered by Thouless in Ref. [16].

Dissipation-free (diamagnetic) currents flow in domains with a potential gradient because the group velocity in such areas is nonzero [see the derivation of Eqn (5)]. In real samples, such areas include:

• incompressible strips at each edge;

• the bulk of the sample. Because the filling factor in the bulk of the sample is an integer, the electronic liquid does not screen the edge potential well, and the potential gradient is nonzero at rather large distances in the bulk of the sample, in contrast to the potential gradient in the model situation shown in Fig. 1;

• regions in the bulk of the sample where the potential has long-period fluctuations. In such inhomogeneities, the same structure of compressible and incompressible strips appears as at the edge.

At equilibrium, when the edges of the sample have equal electrochemical potentials, the total current along an edge is exactly equal to the current along the other edge, but these two currents have opposite directions due to the opposite signs of the potential gradients near the edges [see, e.g., Fig. 1 and Eqn (5)]. The same is true for the bulk current. Circular currents around inhomogeneities do not contribute to the total current through the sample either, and the current therefore vanishes. In the nonequilibrium case (a nonzero difference in the electrochemical potentials of the edges), the current in one direction exceeds the opposite current by exactly the value determined by the difference in the electrochemical potentials of the edges [see Eqn (5)]. This justifies the validity of the Büttiker formalism, which is sensitive only to integral characteristics, such as the electrochemical potentials of the edges and the matrix of scattering coefficients 'from contact to contact.'

A similar situation occurs when equilibrium is absent at only one edge, i.e., when there is a difference in electrochemical potentials for neighboring compressible strips, as shown in Fig. 3. For instance, an increase in the energy of the left compressible strip implies a decrease in its width and a corresponding increase in the width of the incompressible strip. The 'excess' current is determined just by this initially compressible domain, which turns into an incompressible one, and, correspondingly, by the difference in the electrochemical potentials of the strips. Therefore, the 'eternal' question of whether the edge current flows through compressible or incompressible strips can be answered as follows: the current flows through any area with a gradient of the potential, while the nonequilibrium ('excess') current flows along the boundary between compressible and incompressible areas and can be attributed to any of them, depending on whether the areas are considered before or after introducing nonequilibrium conditions.

Taking these considerations into account, we can reformulate the definition of an edge state. In what follows, only *compressible* strips are said to be edge states. This provides a clear definition for the electrochemical potential of an edge state and keeps our consideration consistent with the preceding sections, where an edge state was defined as the intersection of a Landau level with the Fermi level.

The above consideration pertains to the current along the edge of the sample. The current running across the edge and equilibration of the edge states is determined by tunneling through incompressible strips and diffusion in compressible

strips. (The last fact is especially important for complex rearrangements of the edge spectrum, see Section 2.5.)

2.4 The case of strongly nonequilibrium edge states

As mentioned in Section 2.2, studies in the Hall-bar geometry are suitable only in the case of a small imbalance. If the imbalance is large (exceeding the spectral gap values), the parallel channel passing along the edge must be eliminated. In other words, the bar geometry must be replaced by the Corbino geometry. Most probably, a quasi-Corbino geometry in combination with the technique of a crossing gate was first proposed in Ref. [17]. But the first experimental results appeared only ten years later [18], when a measurement method appropriate for obtaining interpretable results was developed and the experimental difficulties arising in such measurements were overcome. (In the geometry originally suggested in Ref. [17], such a measurement method could not be used, which stopped the experimental research.) By that time, the idea of applying the Corbino geometry had been thoroughly forgotten, and the authors of Ref. [18] had to develop the sample geometry anew.

2.4.1 The experimental method. In the quasi-Corbino geometry (Fig. 4), the sample has the shape of a square with an etched domain at the center, which creates two independent boundaries not connected topologically. The two-dimensional electron gas has ohmic contacts on both sides. Just these contacts determine the electrochemical potentials of the boundaries in a quantizing magnetic field. A metal gate surrounds the internal area, leaving free only a T-shaped domain of the two-dimensional gas between the outer and inner boundaries (Fig. 4a). In the regime of the quantum Hall effect with the integer filling factor beneath the gate being less than the integer filling factor in the T-shaped domain, part of the edge states are reflected at the boundary of the gate and are transported along the gate to the other boundary of the sample. At the inner boundary of the sample not covered by the gate (the 'bar' of the T), all edge channels are equilibrated due to the macroscopic size and several ohmic contacts. At the outer boundary of the sample, the area not covered by the gate (the 'leg' of the T), which is called the gate-gap area or the interaction area in what follows, being several micrometers in size (which is much less than the equilibration length at low temperatures), has no ohmic contacts, which considerably hinders equilibration. Thus, if a voltage is applied to a pair of contacts at the inner and outer boundaries, a difference in electrochemical potentials appears between the edge states at the outer boundary of the gate-gap area. The current arising in the gap is the equilibration current for the edge states.

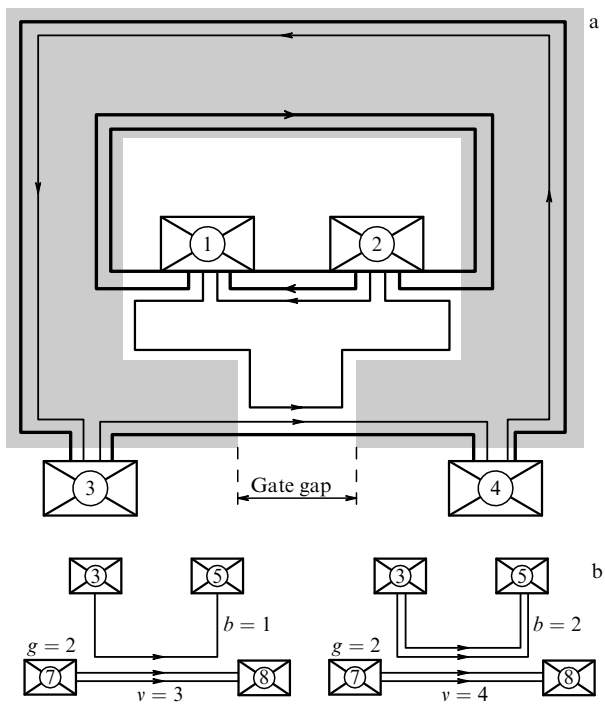

Figure 4. (a) The scheme of a sample in the quasi-Corbino geometry (from Ref. [23]). Bold lines show the inner and outer edges of the mesa, crossed rectangles with numbers denote ohmic contacts, the shaded area is the gate. The structure of the edge states is shown in the case where the filling factor is $g = 1$ beneath the gate and $\nu = 2$ outside the gate. (b) Combinations of various filling factors ($\nu = b + g$) and the edge states in the gate-gap area (from Ref. [18]) — a simplified scheme showing only the states that interact in the vicinity of the gate gap.

In experiments carried out in this geometry, information about the transport is mainly obtained from the current–voltage characteristic (I – V), the dependence of the current between the edge states on the imbalance (voltage) between them. Because of the I – V singularities (see Section 2.4.2), all measurements should be carried out in the DC regime. The unawareness of the necessity for DC measurements, and experimental difficulties arising in DC measurements were the reasons that prevented researchers from obtaining any results before the experiments in Ref. [18].

To measure an I – V, a four-terminal network with a fixed current must be used in most cases. The current between one of the two external contacts and one of the two internal ones (Fig. 4) is fixed with the help of a calibrator, while the remaining pair of contacts is used for measuring the potential difference. (Due to the existence of a preferred direction determined by the magnetic field, there are four principally different combinations of contacts.) Measuring the I – Vs for various combinations of contacts in such a scheme allows detecting and eliminating any possible influence of imperfections of the ohmic contacts on the experimental results.

Preliminary studies of the two-point magnetoresistance between different contacts at the same edge are necessary for estimating the quality of the contacts. For instance, high-ohmic, nonlinear, and Corbino-type contacts can be easily excluded this way. Studying the two-point magnetoresistance between contacts at different edges of the sample provides information about the carrier concentration in the gate-gap area, while the measurement of the magnetocapacitance yields the filling factors available beneath the gate and the degree of homogeneity of the electron system. Such a calibration of the sample, providing the magnetic field and the gate voltage for each pair of the filling factors and specifying reliable ohmic contacts (the total number of ohmic contacts in real samples is much larger than shown in Fig. 4) is performed after each cooling, prior to measuring an I – V, and ensures the reliability and reproducibility of the measurement. The obtained results were qualitatively confirmed by direct measurements of two-terminal I – Vs with fixed voltage.

This geometry offers many degrees of freedom to a researcher. By varying the filling factor in the gate-gap area with the help of a magnetic field, the total number of interacting edge channels can be changed; by varying the

filling factor beneath the gate with the help of the gate voltage, the channels can be divided into groups to which the difference in electrochemical potentials is applied and between which the current flows (Fig. 4). In particular, the transport between edge channels separated by a spin or cyclotron gap or, in double-layer structures, by symmetric–antisymmetric or isospin splitting can be studied.

2.4.2 Transition from the case of a small imbalance to the case of a large imbalance. In the same work [18] where measurements for the strongly nonequilibrium case were performed, transformation of the I–V was demonstrated in the DC measurement. At a high temperature (4 K), the current–voltage characteristics are linear, with the slope exactly corresponding to its equilibrium value obtained from the Büttiker calculation (7) for various combinations of ohmic contacts (Fig. 5). This fact can be explained by the small value of the equilibration length (compared to the size of the interaction area) at this temperature.

We give an example of the Büttiker calculation in the quasi-Corbino geometry for the filling factors $\nu = 4, g = 2$ for the sample shown in Fig. 4. Equations for the currents through the contacts of the sample can be written in the form [see (6)]

$$\begin{aligned} I_1 &= 4\,\frac{e}{h}\,\mu_1 - 4\,\frac{e}{h}\,\mu_2\,, \\ I_2 &= 4\,\frac{e}{h}\,\mu_2 - 2\,\frac{e}{h}\,\mu_1 - 2\,\frac{e^2}{h}(T_{21}\,\mu_1 + T_{23}\,\mu_3)\,, \\ I_3 &= 2\,\frac{e}{h}\,\mu_3 - 2\,\frac{e}{h}\,\mu_4\,, \\ I_4 &= 2\,\frac{e}{h}\,\mu_4 - 2\,\frac{e}{h}(T_{41}\,\mu_1 + T_{43}\,\mu_3)\,, \end{aligned} \tag{9}$$

where I_i is the current coming into or out of the ith contact, μ_i is the electrochemical potential of the ith contact, and $\{T_{ij}\}$ is the explicit form of the transmission coefficients matrix for the transport between edge states in the gate-gap area. The elements of this matrix are not independent: due to the conservation of the total charge in the gate-gap area,

$$\begin{aligned} T_{21} + T_{41} &= 1\,, \\ T_{23} + T_{43} &= 1\,. \end{aligned} \tag{10}$$

Because of the symmetry of the problem, $T_{23} = T_{41}$. Hence, all transmission coefficients can be expressed in terms of a single parameter $T = T_{23}$.

Let the current flow between contacts 4 and 1, with contacts 3 and 2 used for measuring the voltage drop. Then the current flowing through the sample is $I_{41} = I_1 = -I_4$, and the absence of the current through the potential contacts means that $I_2 = I_3 = 0$. The measured voltage drop is the difference in the electrochemical potentials of contacts 2 and 3, i.e., $eU_{32} = \mu_3 - \mu_2$. Solving system (9) and taking relations (10) into account, we find that

$$U_{32} = \frac{2-T}{4T}\,\frac{h}{e^2}\,I_{41}\,. \tag{11}$$

The equilibrium slope is obtained by substituting the equilibrium value $T = 1/2$.

As the temperature decreases to 30 mK, the equilibration length grows dramatically [10], and the system enters the regime of strong nonequilibrium. The current–voltage characteristic becomes essentially nonlinear and asymmetric (see Fig. 5), with a pronounced threshold behavior of the right-hand branch, which becomes linear above the threshold, the left-hand branch remaining nonlinear. A similar transformation of the I–V was observed at low temperatures [19] as a result of varying the length of the interaction area (see Fig. 5). A method for performing such a measurement is described in detail in Section 3.4.3.

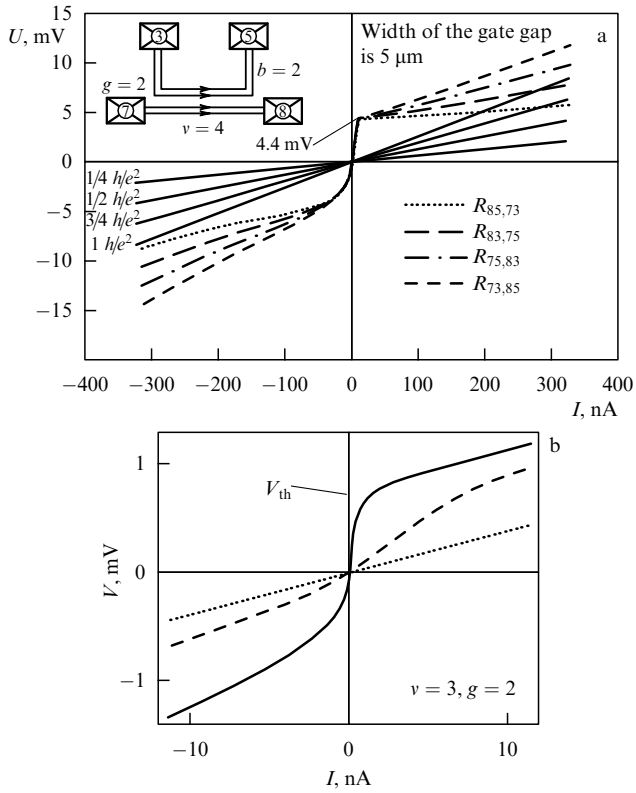

Figure 5. (a) Current–voltage characteristics at a high temperature (complete equilibration) and a low temperature (strongly nonequilibrium regime) for the transport between cyclotron-split edge states (from Ref. [18]). (b) Transformation of the I–V due to the increase in the interaction area for transport between cyclotron-split edge states (from Ref. [19]).

2.4.3 Interpretation of nonlinear current–voltage characteristics. A behavior of the I–V similar to the one described in Section 2.4.2 can only be explained by means of the so-called smooth-edge model, in which the edge is represented by alternating strips of compressible and incompressible electron liquids (Fig. 6). If the filling factor of the sample part not covered by the gate is 2, the interaction area near the outer boundary contains two compressible strips separated by an incompressible strip with the local filling factor equal to 1. The electrochemical potential of each compressible strip is determined by the electrochemical potential of the corresponding (inner or outer) contact.

If a voltage is applied to a pair of contacts corresponding to opposite boundaries, a difference in electrochemical potentials arises between compressible strips in the interaction area. This voltage drops within the incompressible strip between the two compressible ones and affects the distribution of its potential. For instance, at a certain sign of the voltage, the potential barrier between the edge states

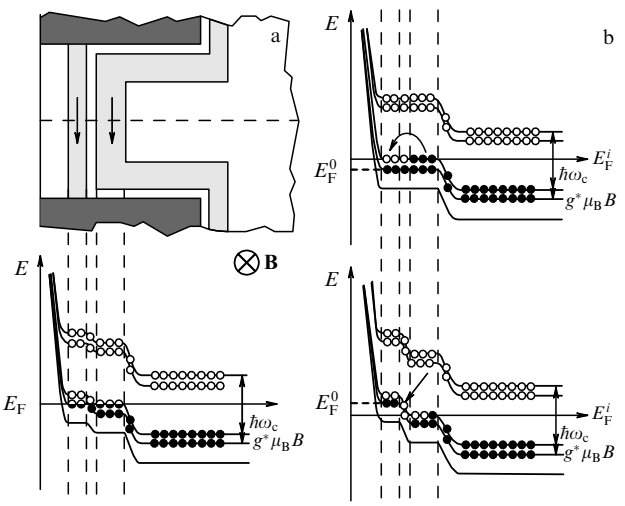

Figure 6. (a) The structure of the sample edge in the interaction area of edge states in equilibrium; the bulk filling factor is equal to 2. Two spin-split energy levels reach the edge and form a structure of compressible and incompressible strips. (b) The structure of the sample edge in the interaction area of edge states in the case of a voltage applied between compressible strips. Under positive voltage, because the electron charge is negative, the potential barrier between the edge states reduces to its value in the case of flat bands. Under negative voltage, the barrier grows and deforms. (From Ref. [18].)

decreases and completely disappears when the voltage is equal to the corresponding spectral gap (see Fig. 6). This leads to a dramatic growth in the current at this voltage and to a complete equilibration between the edge states at large potential differences. At a different sign of the bias voltage, the potential barrier increases, which leads to the appearance of a strongly nonlinear I – V branch.

2.4.4 Spectral studies. Thus, the I – V analysis in this geometry allows the energy gap between the edge states to be found from the position of the threshold voltage on the right-hand (positive) I – V branch. It turns out that the gap is equal to the bulk value of splitting between the corresponding energy levels. This fact was first demonstrated for cyclotron gaps [18], which justifies using the smooth-edge model and experimentally confirms the smoothness of an etched edge in the IQHE regime. All reasoning concerning the I – V must also be valid in the case of a sharp edge, with the difference that the measured gap is then much larger than the bulk value of the splitting (see Section 2.1.2, where definitions are given for smooth and sharp edges). For sufficiently pure samples, it was shown in [20] that the gap between spin-split edge states corresponds to the bulk exchange-increased Lande factor [21].

2.4.5 Equilibration at the edge. In addition to spectroscopic studies, the authors of Ref. [22] studied the process of equilibration, with the initial values of imbalance exceeding the spectral gap in the transport between cyclotron-split edge states. In experiment, the slope of the linear (above-threshold) part of the I – V right-hand branch was studied (Fig. 7). It turned out that for strongly nonequilibrium edge states, not the whole difference of electrochemical potentials but only the part exceeding the spectral gap can be redistributed. The authors also modified the Büttiker formalism by explicitly introducing a local characteristic of

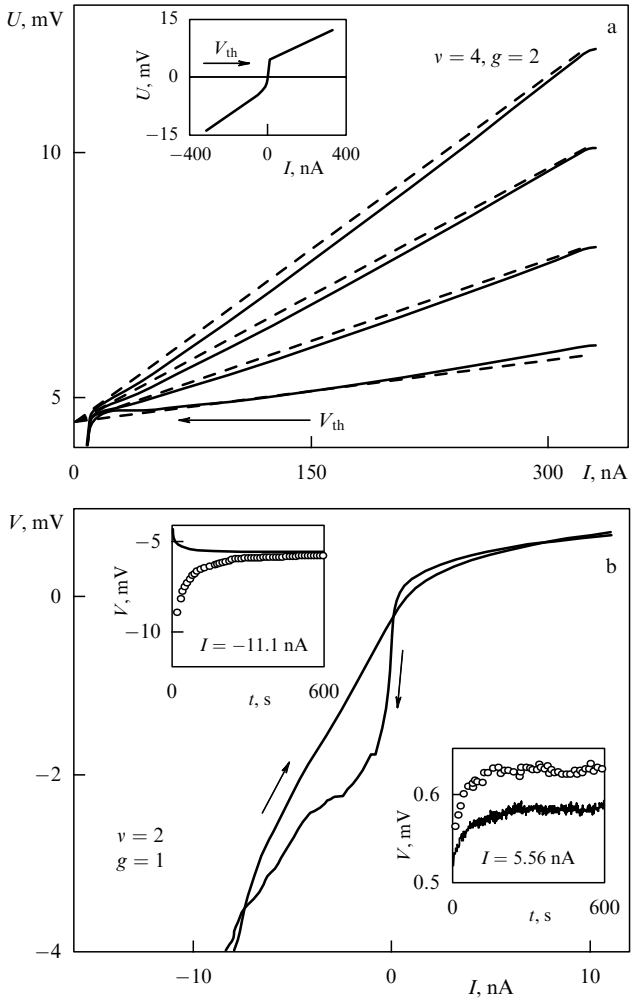

Figure 7. (a) Slopes of the linear parts of current – voltage characteristics (solid lines) for various combinations of contacts and their fitting (dashed lines) using a single parameter α (from Ref. [22]). The inset shows the shape of the total current – voltage characteristic for transport between the edge states separated by a cyclotron gap. (b) Hysteresis on the I – V for the spin-flip transport and relaxation curves (from Ref. [23]).

the transport between the edge states instead of the matrix T_{ij} with integral entries. Namely, the parameter α was defined as the ratio of the difference in electrochemical potentials passed between the edge states and the difference in electrochemical potentials allowed for redistribution.

We demonstrate how this parameter can be introduced for the sample shown in Fig. 4. At a voltage below the threshold, the current between the edge states in the gate-gap area is virtually absent. This means that the edge states leave the gate-gap area with the initial electrochemical potentials μ_1 and μ_3. At a voltage above the threshold, a current between the edge states occurs; hence, only a part of the initial electrochemical potential difference, $\mu_3 - \mu_1 - eV_{th}$, can be redistributed. We introduce a parameter α showing what part of this difference is actually transferred in the gate-gap area: $\alpha(\mu_3 - \mu_1 - eV_{th})e/h$. The parameter α is easy to interpret. Indeed, for the combination of filling factors $\nu = 4$ and $g = 2$, a complete equilibration corresponds to the distribution of $\mu_3 - \mu_1 - eV_{th}$ in two equal parts, i.e., $\alpha = 1/2$. Edge states leave the interaction area with the electrochemical potentials $\mu_1 + \alpha(\mu_3 - \mu_1 - eV_{th})$ and $\mu_3 - \alpha(\mu_3 - \mu_1 - eV_{th})$. Then the

Büttiker system of equations (9) can be written as

$$
\begin{aligned}
I_1 &= 4\,\frac{e}{h}\,\mu_1 - 4\,\frac{e}{h}\,\mu_2\,,\\
I_2 &= 4\,\frac{e}{h}\,\mu_2 - 2\,\frac{e}{h}\,\mu_1 - 2\,\frac{e}{h}\left[\mu_1 + \alpha(\mu_3 - \mu_1 - eV_{\rm th})\right],\\
I_3 &= 2\,\frac{e}{h}\,\mu_3 - 2\,\frac{e}{h}\,\mu_4\,,\\
I_4 &= 2\,\frac{e}{h}\,\mu_4 - 2\,\frac{e}{h}\left[\mu_3 - \alpha(\mu_3 - \mu_1 - eV_{\rm th})\right].
\end{aligned}
\tag{12}
$$

Solving system of equations (12) for the combination of contacts used in calculating (9), we obtain the relation

$$U_{32} - V_{\rm th} = \frac{2-\alpha}{4\alpha}\,\frac{h}{e^2}\,I_{41}\,. \tag{13}$$

We note that relation (13) describes the current at a voltage exceeding the threshold one. Hence, for a constant slope of the linear positive branch of the I – V shown in Fig. 7, the parameter α is constant, in contrast to the corresponding Büttiker coefficient T, which is nonlinear whenever the I – V is nonlinear.

This single parameter α is universal: it fully describes the slopes of linear parts of the I – V for any combination of the contacts (see Fig. 7) and depends only on the physics of the transport between edge states. Numerical values of α indicate the extent to which equilibrium is established between the edge states.

2.4.6 Spin-flip transport: creation of dynamic nuclear polarization. The transport between spin-split edge states should be accompanied by the electron spin flip. The spin flip is mainly provided by the spin – orbital interaction [10], but part of the electrons participate in the so-called flip-flop process: due to the hyperfine interaction, the spins of the electron and the nucleus are flipped simultaneously. This process, even at relatively high temperatures, leads to the creation of an area with the dynamic polarization of nuclear spins, in which the static polarization by the external magnetic field is inessential [12, 13].

Creation of dynamic nuclear polarization has been studied in the strongly nonequilibrium case in Ref. [23], where the I – Vs were measured for the transport between spin-split edge states in the quasi-Corbino geometry. Under these conditions, current – voltage characteristics exhibit a considerable hysteresis, especially pronounced in the left-hand (negative) branch (see Fig. 7). Comparison with the I – V obtained for transport without the spin flip (through a cyclotron gap) in the same field and with the same degree of disorder showed that the hysteresis is not related to the slow recharging of the sample from the contacts. It was shown in Ref. [23] that the hysteresis is caused just by the dynamic polarization of the nuclei in the interaction area of the sample. Indeed, the effective Overhauser field arising in this case influences the spin splitting, which determines the potential barrier between the edge states. This has an impact on the current for all electrons, and not only for those whose spin flipping is caused by the flip-flop process; as a result, a noticeable hysteresis of the I – V occurs.

In addition, relaxation processes investigated in Ref. [23] (see the inset in Fig. 7) revealed two typical relaxation times, of the order of 25 and 200 s. The first time corresponds to the creation of the dynamic nuclear polarization area at a certain stage of the transport between the edge states, and the second relates to the development of a stable area where nuclear spins in the sample are polarized due to the competition between the nuclear spin diffusion and the escape of the spins from the system.

2.5 Edge states in double quantum wells

More complicated for investigation are tunnel-coupled double electron layers, or double-layer systems, which are usually realized in double quantum wells separated by a tunnel-transparent barrier (Fig. 8) or in broad quantum wells where layering occurs due to Coulomb repulsion. Because of the tunneling between the layers, the bulk spectra of such systems are already rather complicated.

The simplest system is a symmetric double quantum well. In this case, symmetric – antisymmetric splitting occurs even in a zero magnetic field, due to the lifting of the double degeneracy of energy levels in two identical tunnel-coupled quantum wells. The degeneracy is lifted because of the creation of two common energy subbands with the spatially symmetric and antisymmetric wave functions. It is the energy difference in these subbands that is called the symmetric – antisymmetric splitting.

In unbalanced double-layer systems, each layer has its own ladder of Landau levels [24]. In smooth systems, where the charge transfer between the layers leads to an essential

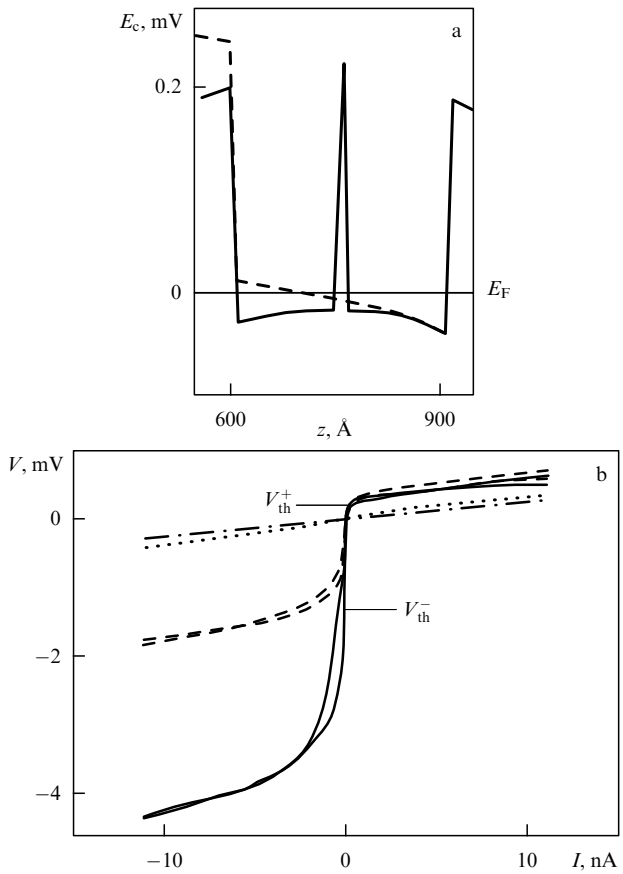

Figure 8. (a) Profile of a double quantum well with a narrow tunnel barrier in the symmetric and asymmetric cases (from Ref. [36]). (b) Transformation of the current – voltage characteristic for transport between spin-split edge states in a double-layer system when approaching the bulk phase transition point: from being strongly nonlinear, the I – V becomes almost linear and the hysteresis disappears (from Ref. [33]).

rearrangement of the energy levels, a quantizing magnetic field can cause hybridization of the layers and create common subbands, similarly to the symmetric case with a zero magnetic field [25]. But if the magnetic field is introduced in the plane of the two-dimensional system, the wave functions of different layers become nonorthogonal to each other even for different orbital quantum numbers, which leads to the creation of common subbands at all filling factors in any (quantizing) magnetic fields [26]. For the description of such effects, it is useful to introduce a new quantum number, the isospin, which is equal to $\pm 1/2$ for an electron that totally belongs to one of the electron layers. Hybridization of the layers and the creation of subbands lead to the mixing of these states [25].

At the edge of the sample, the Fermi level becomes the same for edge states that originate, in the general case, from different parts of the quantum well or from subbands, depending on the quantum well symmetry. Energy levels differing in the new quantum number, the isospin, can form a rather complicated structure at the edge and even overlap. In this case, it is impossible to predict even the systematization of the edge states, to say nothing of the transport between them. Investigation of this problem is extremely important both in and of itself and because of the numerous experiments on the inter-layer drag, in which the effect of transport at the edge is usually ignored.

2.5.1 Transformation of the edge-state structure during a phase transition in the bulk of the sample. In the symmetric case, in addition to the cyclotron and spin splitting, a symmetric – antisymmetric splitting appears, which is smaller than the Zeeman splitting in strong fields and exceeds it in weak fields [27 – 29]. In intermediate fields, where these splitting values should be comparable, a new phase, the so-called antiferromagnetic one, appears due to the electron – electron interaction [30 – 32]. A bulk transition into this phase from the range of weak fields was observed in Ref. [29] and from the range of strong fields in Ref. [28]. Thus, singularities can be expected in the transport between edge states in the vicinity of the bulk phase transition point.

Such transport singularities were observed in Ref. [33], where the incompressible strip separating edge states was demonstrated to disappear near the bulk phase transition point (see Fig. 8). Disappearance of the I – V hysteresis, which is observed far from the phase transition and is typical for the transport between spin-split edge states, also indicates that the potential barrier between the edge states disappears near the bulk phase transition point, because the hysteresis is related to the effect that the effective Overhauser field has on the potential barrier (see Section 2.4.6).

An important fact following from this observation is that the structure of edge states always corresponds to the structure of the bulk spectrum and follows even its complicated transformations.

2.5.2 Realization of topological defects in the structure of edge states. The Pauli principle does not forbid the intersection of edge states corresponding to different quantum numbers. For example, Fig. 9 shows the intersection of spin-split edge states. Such intersections were called defects in the topological structure of edge states, or topological defects. The possibility of the existence of such defects was proved theoretically in Refs [34, 35]. The experimental realization and observation of such defects still remains a problem. In particular, the intersections shown in Fig. 9 can have no effect on the transport between edge states: intersection in space does not influence the spin flip, which determines the transport between spin-split edge states.

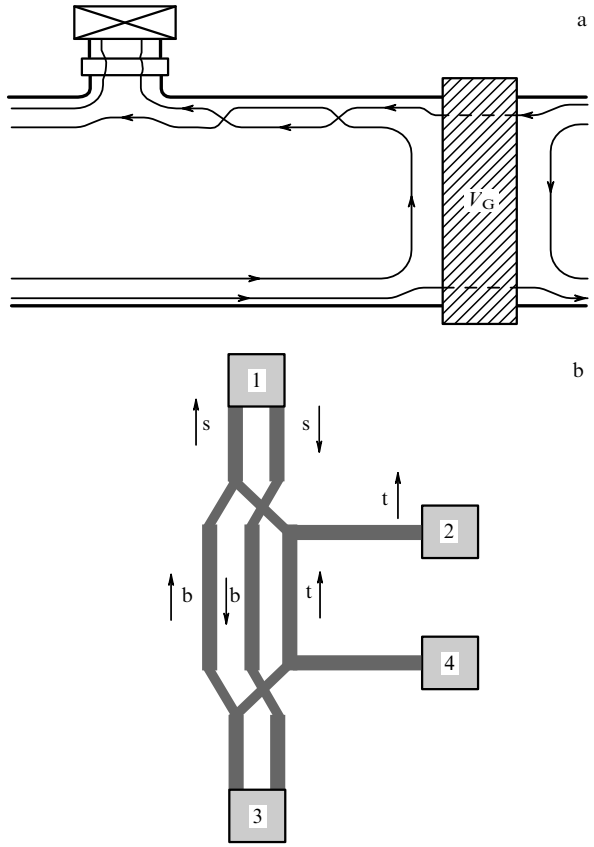

Figure 9. (a) The simplest example of topological defects in the structure of edge states. (From Ref. [35].) (b) Realization of topological defects in the structure of edge states. Edge states coming from beneath the gate are spin-split and mixed (symmetric) with respect to isospin (s denotes the symmetric state and t and b the top and bottom layers). Because of the initial asymmetry of the quantum well, the edge states in the interaction area are split in both spin and isospin. Spin and isospin conservation leads to a transformation of the structure of edge states near the gate boundary and to their intersections, which are topological defects. (From Ref. [36].)

Nevertheless, the only way to detect topological defects is by studying the transport between edge states, which can be most conveniently done in the quasi-Corbino geometry [18]. The existence of a gate in this geometry, in particular, allows changing the symmetry of the quantum well, and hence the energy spectrum, beneath the gate. Since the structure of edge states corresponds to the structure of the bulk spectrum, the quasi-Corbino geometry allows realizing topological defects in the structure of edge states [36].

If the well is asymmetric in the interaction area of the edge states, then edge-state electrons are fully described by the spin and isospin orientations. Electrons injected from beneath the gate can come either from an isospin-polarized state or from a mixed one. In the latter case, because the injection occurs with isospin conservation, the electrons are distributed among the edge states. This results in the intersections of edge states (see Fig. 9) — the topological defects — and in the equilibration of electrochemical potentials for all edge states in the interaction area, which manifests itself in the perfect linearity of the I – V in a normal magnetic field (Fig. 10). If a tangential field is

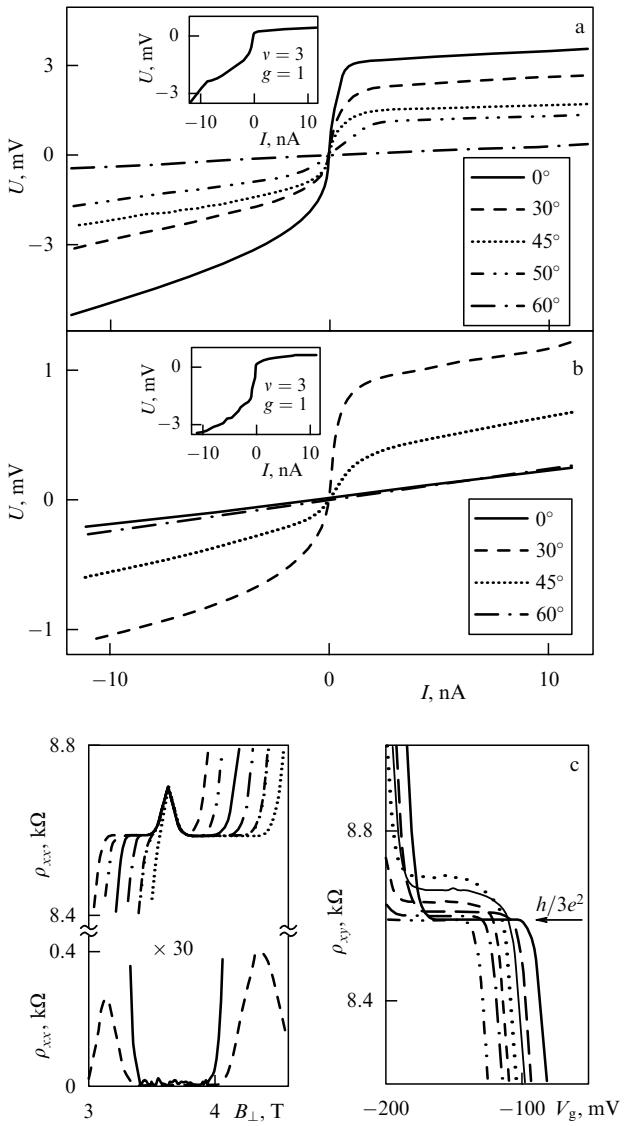

Figure 10. Experimental manifestation of topological defects in the structure of edge states: (a) the I–V of a sample having no topological defects in the structure of edge states in a normal magnetic field; (b) transformation of the I–V due to the appearance and disappearance of topological defects in the interaction area: the initially linear I–V jumps to being strongly nonlinear and is then slowly transformed into being weakly nonlinear (from Ref. [36]); (c) shift of the Hall plateau level while maintaining the dissipation-free regime, as an example of the influence of topological defects on the transport in double-layer structures (from Ref. [37]).

applied, the states in the interaction area become isospin-mixed, and the topological defects disappear. This leads to a strongly nonlinear I–V, usual for this situation. A further increase in the tangential field reduces the spectral gaps in the bulk, which, in turn, reduces the gap between the edge states (as can be seen from the reduction in the I–V threshold) and also influences their topological structure. In this way, the existence of topological defects and the possibility of controlling their creation and disappearance were demonstrated in Ref. [36].

An example of the possible influence of topological defects is given in Ref. [37], where a shift in the Hall plateau without the appearance of the dissipative resistance component was discovered in certain regions of the phase diagram (see Fig. 10) via high-precision measurements of the resistance tensor components for a double-layer system in the IQHE regime. Such a shift can only be explained by the disappearance of edge equilibration in the corresponding regions of the phase diagram, because bulk inter-layer transport is forbidden in these regions [25].

2.6 Collective excitations at the edge

Investigation of collective excitations began almost immediately after the start of research on two-dimensional electron systems. Similarly to the three-dimensional case, collective modes in two-dimensional systems in the absence of a magnetic field are plasma oscillations, plasmons, having a typical plasma frequency. In a quantizing magnetic field (i.e., in the IQHE regime), such oscillations are called magnetoplasmons because of the dependence of their spectrum on the magnetic field. Finally, in the presence of a boundary, a new branch of magnetoplasmon excitations appears, the edge magnetoplasmon, whose spectrum is gapless. Although edge magnetoplasmons, like any plasma oscillations, do not transfer charge, they have a considerable effect on the transport properties of two-dimensional systems.

2.6.1 The spectrum of edge magnetoplasmons. The most complete theoretical investigation of edge magnetoplasmon spectra for various experimental geometries (a disc, a half-plane, a narrow bar with or without a metal gate) has been carried out in Ref. [38]. In all cases, the spectrum turned out to be gapless and, as a rule, nearly linear, $\omega \sim k$. In systems with a metal gate, electric fields are screened at distances comparable to the distance to the gate, which leads to a perfectly linear dispersion law. For instance, for a half-plane with a gate, the dispersion law is

$$\omega = 2\pi\sigma_{xy}k\sqrt{\frac{d}{l}}\,, \tag{14}$$

where σ_{xy} is the Hall conductance and d and l are the distance to the gate and the width of the charge accumulation area, respectively. Thus, edge magnetoplasmons are long-lived charge fluctuations at the edge of the sample (Fig. 11) moving along the edge with the group velocity $v = \mathrm{d}\omega/\mathrm{d}k$. Their propagation velocity is determined by Hall's component of the conductance and their dissipation is determined by the conductance dissipative component, which tends to zero in the IQHE regime.

The study of edge magnetoplasmons is apparently interesting both in and of itself and from the standpoint of investigating complicated edge structures. On a smooth edge,

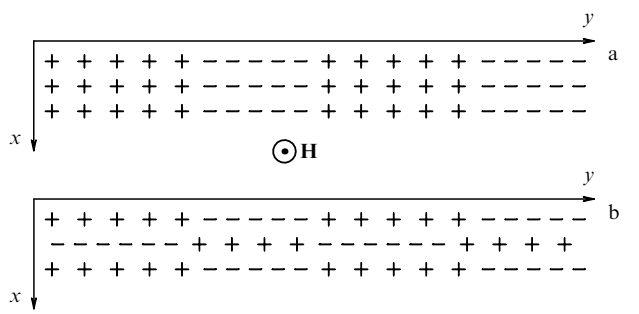

Figure 11. Long-lived charge fluctuations at the edge of a sample in the IQHE regime — edge magnetoplasmons: (a) basic (charged) mode, (b) neutral mode. (From Ref. [43].)

charge accumulation can occur only in compressible strips, which is theoretically predicted to make the propagation velocity of the excitations depend on the real structure of the edge [for instance, via the width l of the charge accumulation area in Eqn (14)].

2.6.2 Experimental observation. Experimental research on edge magnetoplasmons started with resonant measurements in the frequency domain [39], which proved the existence of such excitations and revealed their spectrum and damping. But these studies did not show any dependence of the spectrum on the structure of the edge.

Another approach to the study of edge magnetoplasmons is via time-resolved measurements of the propagation of edge-magnetoplasmon wave packets [40–42]. In these experiments, the value under study was the potential establishing rate at the edge of the sample, $v = \mathrm{d}\omega/\mathrm{d}k$, which was the same for all k in structures with gates. A stepwise potential was applied to one of the potential contacts, and the potential at the other contact was measured as a function of time. An advantage of this method is its high sensitivity: there is ideal coupling between the emitter and the system under study, on the one hand, and between the system under study and the receiver, on the other hand. This is very important for measurements near the metal gate. The gate allowed varying the filling factor (the number of strips at the edge) and screened the electric fields, which made the charge accumulation area of edge magnetoplasmons shrink to the size of the edge area. A qualitative result of these experiments is shown in Fig. 12: a potential jump applied to a contact led to edge-magnetoplasmon wave packets propagating along the edge and establishing the edge potential [41]. The number of packets and their velocities are determined by the number and width of compressible strips at the edge. Simultaneously with the establishing of the edge potential (with the typical time σ_{xy}^{-1}), there is a flow of current into the bulk of the sample, which, however, occurs on a much larger time scale:

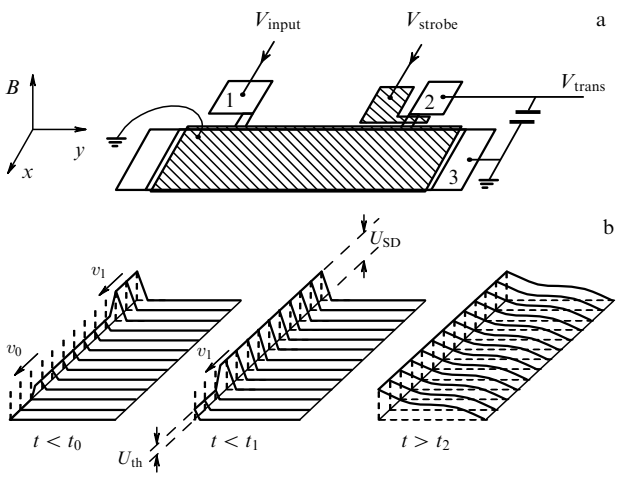

Figure 12. (a) Study of the propagation velocity of edge magnetoplasmon wave packets. A rectangular voltage pulse is applied between contact 1 and the ground (contact 3). The voltage amplitude at contact 2 is measured as a function of time. The main gate is for varying the filling factor of the two-dimensional electron gas and for screening electric fields; the additional gate is for suppressing parasite signals. (From Ref. [42].) (b) Establishing the edge potential: spreading of edge-magnetoplasmon wave packets over edge states and their further propagation into the bulk of the sample. U_{SD} is the bias (source-drain) voltage. (From Ref. [41].)

the rate is determined by the value σ_{xx}, which is small in the IQHE regime, $\sigma_{xx} \ll \sigma_{xy}$. Thus, collective excitations at the edge are responsible for the establishing of the edge potential.

2.6.3 Neutral modes: theory and possibility of experimental observation. In addition to the basic mode of edge excitations, which was described in Section 2.6.2, other edge modes may exist, in which the charge density varies not only along the edge but also in the orthogonal direction (Fig. 11b). Such modes have been predicted theoretically [43] and called neutral (because of the possible mean neutrality of the charge at the edge), or acoustic, modes. They can be excited, for instance, as follows. Collective excitations are studied within a narrow strip of two-dimensional gas. Then the usual modes of edge magnetoplasmons existing near the edges cannot be considered independent because the fields formed by them affect each other and the modes form a joint neutral excitation. If several strips are close to each other, as is the case on a smooth edge, oscillation of the mode charge occurs in the direction orthogonal to the edge of the sample (Fig. 11b).

It is precisely because of the neutrality of their mean charge that neutral modes cannot be discovered in experiments as described above. Such attempts have been made, for instance, via inductive excitation of edge magnetoplasmons [44] on an etched mesa boundary. The excited magnetoplasmon was supposed to further propagate along the interface of two filling factors created by the gate. An edge magnetoplasmon should propagate along such a boundary within a narrow strip, which could lead to the excitation of a neutral mode in that strip. In spite of the record-breaking sensitivity of the experimental setup, no conclusion could be made about the existence of the neutral mode.

Investigation of neutral modes is important not only in and of itself. These modes are responsible for the potential establishing at the edge when the charge is redistributed through incompressible strips of a two-dimensional system, i.e., for the tunnel density of states. In the IQHE regime, charge redistribution is mainly determined by the single-particle transmissivity of the tunnel barrier and its dependence on the bias voltage. This transmissivity makes an exponential contribution to the transport current (see Section 2.4.3). The tunnel density of states is then given by the pre-exponential factor and it is therefore almost impossible to measure it experimentally. Nevertheless, in the FQHE regime, where the spectral gaps are small, effects of neutral modes become important, as we show in Section 3.4.4.

2.7 Basic conclusions for the integer quantum Hall effect

We summarize the results of studying edge states in the IQHE regime.

• The edge potential of a real system can be considered smooth. At the edge, there is a structure of compressible and incompressible strips of electron liquid, corresponding to the energy level structure in the bulk of the sample.

• The Büttiker formalism is sensitive only to integral values, such as the electrochemical potentials of the edges and total scattering between the edge states. Therefore, it correctly describes the current along the edge in the IQHE regime and allows taking the current redistribution between edge states into account.

• For both large and small imbalances between edge states, equilibration occurs by means of the electron transport through incompressible strips. This process is fully

governed by the single-particle tunnel transparency of the barrier in such strips and by its independence of external parameters.

• At the edge, there exist long-lived gapless collective excitations (edge magnetoplasmons) whose spectrum corresponds to the structure of strips in the electron liquid. In the IQHE, it is not possible to observe the excitation of neutral collective modes.

• The structure of edge states for double-layer tunnel-coupled systems corresponds to the structure of the bulk spectrum and even follows its considerable rearrangements. This leads to a possibility of topological defects appearing in the edge states. In the analysis of transport experiments in double-layer systems, transport effects between edge states must necessarily be taken into account.

3. Edge states in the fractional quantum Hall effect

As mentioned in the Introduction, studies in the fractional quantum Hall effect regime mean studies in the regime of strong interaction. Correspondingly, investigation of edge states implies that the interaction is consistently taken into account, which considerably complicates the problem. Indeed, many experimental results obtained in this field are still waiting for explanation and, at the same time, many theoretical predictions have not yet been verified in experiment. Here, the discussion includes only the results that are reliably observed in experiment.

3.1 Present interpretation of the fractional quantum Hall effect

In the fractional quantum Hall effect regime, the system consists of a large number of strongly interacting particles, and therefore no method exists for exactly solving the problem with the real Hamiltonian. The interaction results in a rearrangement of the ground state of the system of particles, and the new state cannot be obtained from the perturbation theory as a small correction to the interaction-free state. Rather long ago, it became clear that the new ground state is not a Wigner crystal with a long-range order. Indeed, such a state would be pinned with impurities, with the result that a finite Hall conductance would be impossible. The new ground state is rather that of a strongly interacting quantum liquid. Two approaches turned out to be efficient for the description of such a liquid: the mean-field method (based on the hypothesis of composite fermions) and the method of a trial ground-state wave function (the Laughlin approach). The second method proved to be the most productive for the theory of the fractional Hall effect, and we consider it first.

3.1.1 Laughlin's variation function. Laughlin [45] proposed to describe the ground state in the FQHE regime at $\nu = 1/3$ by means of the wave function

$$\Phi_m(z) = \prod_{i<j}(z_i - z_j)^m \prod_k \exp\left(-\frac{|z_k|^2}{4l_{\mathrm{H}}^2}\right), \tag{15}$$

where $z_i = x_i - \mathrm{i}y_i$ is a complex coordinate of the particle (in the plane) and l_{H} is the magnetic length.

Wave function (15) has the following advantages:

• at $m = 1$, it is the exact wave function of a completely filled lowest Landau level;

• for odd m, due to the existence of the exponential factor $(z_i - z_j)^m$, it is antisymmetric with respect to the permutation of any two particles, i.e., it takes fermionic statistics into account;

• it tends to zero when the particles approach each other (the exponent m gives the rate of tending to zero) and takes the dynamic repulsion of particles into account; and

• it is exact for systems with small numbers of particles ($N = 3-10$), which is confirmed by numerical simulations.

Assuming the ground-state wave function to have form (15), Laughlin carried out a variational calculation of the ground-state energy for fractional filling factors of the form $\nu = 1/(2k+1)$, $k = 1, 2, 3, \ldots$ (the so-called principal Laughlin sequence), with m being the variation parameter. It turned out that

• the ground-state energy is minimal for $m = 1/\nu = 3, 5, 7, \ldots$ and is then much lower than the ground-state energy of a Wigner crystal;

• elementary excitations are separated from the ground state by a gap with the typical energy $0.1e^2/\varepsilon l_{\mathrm{H}}$, where ε is the dielectric permittivity;

• elementary excitations have the charge $e/m = e\nu$; and

• from excitations with a given odd m, daughter ground states with a larger odd m can be constructed. This way, the hierarchy of states in the FQHE regime is partly explained.

In Laughlin's theory, this last result is the most difficult to understand but it suggests a way of testing the theory: it implies that if the FQHE is observed for 'fifths' fractional filling factors, $\nu = n/5$, $n = 1, 2, 3, 4$, it must be observed for 'thirds' as well. The inverse statement is not true in general. This fact is always confirmed in experiment: as the purity and homogeneity of a two-dimensional system improves, first the 'thirds' FQHE is manifested, then 'fifths,' then 'sevenths,' etc.

Another prediction of Laughlin's theory that allows an independent verification is the symmetry between the ground states for the filling factors ν and $1 - \nu$. In particular, the ground state for the filling factor $\nu = 2/3$ can be built as the ground state for holes with the filling factor $\nu = 1/3$ on the background of a completely filled lowest Landau level. This state can be either spin-polarized or spin-nonpolarized [46]. In weak magnetic fields, the spin-nonpolarized ground state is advantageous in terms of energy, while the spin-polarized state is more advantageous in strong fields. Therefore, an increase in the magnetic field should lead to a phase transition from the spin-nonpolarized state into a spin-polarized one.

Such a phase transition has indeed been observed experimentally [47]. In Fig. 13, we show how the FQHE state for $\nu = 2/3$ disappears and then reappears as the magnetic field increases. Some of the most recent results in this field were obtained in Ref. [48], where this phase transition was studied in comparison with the phase transition to the tilted antiferromagnetic phase [30], also caused by the electron – electron interaction. Comparing the behavior in both phase transitions, one could conclude that the phase transition between the FQHE states occurs through the evolution of the domain structure near the phase transition point.

3.1.2 Hypothesis of composite fermions. Another approach to the description of the system in the integer Hall effect regime is the hypothesis of composite fermions [49]. We consider the

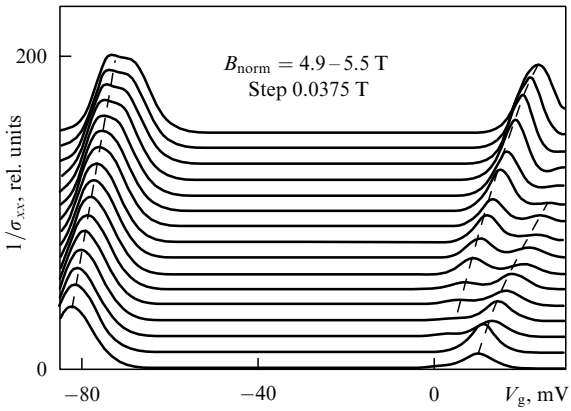

Figure 13. Phase transition from the spin-nonpolarized ground state to the spin-polarized one as a result of the magnetic field increase. The measured parameter is the dissipative conductance component. In the right-hand part of the figure, the FQHE state with $\nu = 2/3$ can be seen to disappear and then reappear, the two states coexisting within some range of magnetic fields and concentrations. In the left-hand part of the figure, the peak for $\nu = 1/3$ is monotonically increasing. (From Ref. [48].)

Hamiltonian of a system of interacting electrons

$$H = \sum_{i=1}^{N} \frac{\left(p_i + (e/c)A_i\right)^2}{2m_{\rm b}} + \sum_{i \neq j} V(r_i - r_j) + \sum_{i=1}^{N} U(r_i)\,, \quad (16)$$

where the first and the last terms describe the motion of a single electron in the magnetic field and an external scalar potential (see Section 2.1.1) and the second term describes pair interactions between electrons; $m_{\rm b}$ is the band mass. Clearly, it is impossible to find the exact solution of the Schrödinger equation with such a Hamiltonian for a large number of particles.

The idea of the method is to replace the interaction term by a fictitious vector potential acting on the electrons and then to take the *mean* value of this field. (The potential must be a vector one in order to maintain the antisymmetry with respect to pairwise permutations of the particles.) Thus, the problem is reduced to the consideration of a *single* particle in the mean field created by all other particles. The model Hamiltonian is written as

$$H_{\rm CF} = \frac{\left(p + (e/c)A - (e/c)\langle a(r)\rangle\right)^2}{2m_{\rm b}} + U(r)\,, \quad (17)$$

where $\langle a(r)\rangle$ is the mean value of the fictitious vector potential. We note that this Hamiltonian is already a single-particle one and permits an exact solution (known as the Landau quantization). It is important to note that the transformation used here does not change the effective mass: it remains the band mass.

The considered transition to a model Hamiltonian means, in fact, that to each electron we 'attach' two quanta of magnetic flux directed oppositely to the external field; the motion of such a particle (the composite fermion) is considered in the mean field of all other particles and the external magnetic field. As a result, new particles move in the effective magnetic field $B^* = B(1 - 2\nu)$, their Landau levels are separated by the 'cyclotron' gap $\hbar e B^*/(m_{\rm b} c)$, and the fractional Hall effect can be described as the integer quantum Hall effect for composite fermions. The filling factors of electrons and composite fermions are related as $p = \nu/(1 - 2\nu)$, $p = 1, 2, \ldots$.

Among the advantages of the composite-fermion theory, there are the simplicity of explaining the hierarchy of the FQHE levels, the simplicity of introducing the spin (as an additional Zeeman splitting of composite fermion levels) and, most importantly, the introduction of a new typical size parameter, the inverse Fermi momentum, which is revealed in focusing experiments [50]. The last fact has still not been explained in the framework of the Laughlin theory.

As drawbacks of the composite-fermion theory, we mention the wrong scale of the excitation energy in the FQHE regime (the cyclotron energy of composite fermions) and the introduction of a new energy scale, the Fermi energy of composite fermions, which so far has not manifested itself in experiment. The first problem is usually 'coped with' by introducing the effective mass of composite fermions, to make the excitation energy behavior conform to the Laughlin theory. (It is easy to see that in this case, the effective mass scales as the square root of the magnetic field.) Unfortunately, this method cannot be justified in the framework of the composite-fermion approach, which makes this model inconsistent at the very least.

Even if the theory of composite fermions is used with the excitation energy obtained in the Laughlin theory, there still remains a qualitative difference between these two theories. Namely, in the Laughlin approach, there is only the ground-state energy below the Fermi level, while in the theory of composite fermions, several filled levels lie below it, i.e., there are spectral *gaps* below the Fermi level. The absence or presence of gaps below the Fermi level can be discovered experimentally, and the results of such an experiment would be serious evidence either in favor of the composite-fermion hypothesis or against it. So far, there is no such evidence, and the only complete theory of the FQHE remains the method of Laughlin's wave function, which is used in the present review as the basic one. Nevertheless, due to the simplicity and beauty of the composite-fermion hypothesis, we also make comments using this simple 'single-particle' language.

3.2 Edge states: the case of a sharp potential

To introduce edge states, we first consider the simplest case, that of an infinitely sharp edge potential. This case is interesting not only as a way to introduce edge states (as for the IQHE) but also from the experimental standpoint, because it can be realized in practice.

3.2.1 Transport along the edge and the structure of edge states. MacDonald [51] has shown that the energy of the ground state in the FQHE grows when approaching the edge of a system with an infinitely sharp potential, and an edge state appears at the intersection with the electrochemical potential level. The nonequilibrium current, similarly to the case of the IQHE, can be written in terms of the electrochemical potential difference for edge states: $I = (e^*/h)\Delta\mu$, where $e^* = e\nu$ is the effective charge in this FQHE state. But this description is valid only for simple states from the principal Laughlin sequence, having filling factors of the form $\nu = 1/3, 1/5, 1/7, \ldots$. For other filling factors, the picture at the edge is more complicated. For instance, the state with $\nu = 2/3$, according to Laughlin [45], is constructed as a hole state on the background of a completely filled lowest Landau level. Correspondingly, in this case, edge states for electrons with integer charge (from the filled Landau level) coexist with

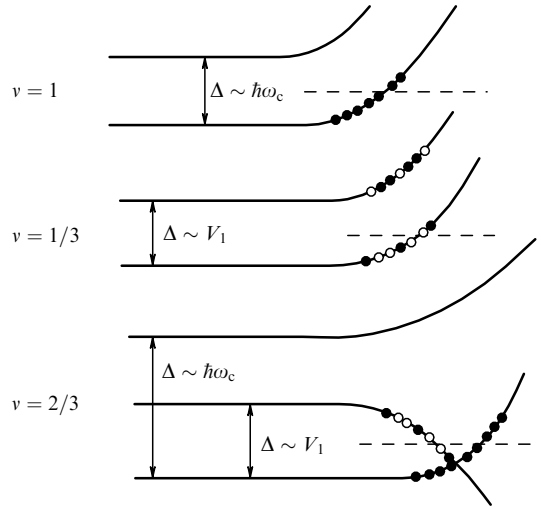

Figure 14. The emerging of edge states in the case of an infinitely sharp edge potential for the filling factors 1, 1/3, 2/3. (From Ref. [51].)

edge states for holes with fractional positive charge [51] (Fig. 14). The total edge current is determined by the sum of currents for all edge states. It is then possible to introduce the transmission coefficient matrix and thus accomplish the construction of the Büttiker formalism for the FQHE [51].

Although this formalism yields correct results for the resistance of the sample in the FQHE regime at various combinations of current and potential contacts, its basic prediction, the existence of a complicated structure of edge states for filling factors different from the ones of the Laughlin principal sequence, requires independent experimental verification. Direct testing in experiments with a crossing gate is impossible because of the smoothness of the electrostatic gate potential. The only experimental evidence of the existence of such a structure is given in Ref. [20], which is described in detail in Section 3.4.2.

The same results follow rather naturally in the approach of composite fermions [52] whose Landau levels, being equidistant in the bulk of the sample, bend upwards near the edge of the sample. The number of levels (i.e., the number of edge states) is determined by the number of Landau levels for composite fermions, i.e., by the given fractional filling factor. For instance, there is one state for 1/3 and two for 2/3, in full agreement with MacDonald's result [51]. Calculation of the current over the edge states [52] is in this case somewhat more difficult (because of the difference between the chemical potentials of electrons and composite fermions) but leads to the same results.

3.2.2 Collective modes and tunneling into the edge. An important and interesting question is the one about the collective excitations at the edge of the system in the FQHE regime, in which, unlike in the IQHE case, the inter-electron interaction must be consistently taken into account. This was done in the theoretical works by Wen [6], who applied the Luttinger model of a one-dimensional interacting liquid [5] to this problem and demonstrated that collective excitations with a gapless spectrum must exist at the edge. Physically, these excitations correspond to different modes of edge magnetoplasmons. We note that an edge state in the FQHE regime is probably the only exact realization of a chiral (directed) Luttinger liquid: the edge creates the one-dimensionality of the system, bulk states form an infinite reservoir, which is necessary in the Luttinger model, and the magnetic field determines a preferred direction providing the chirality of the electron liquid. Therefore, the investigation of collective excitations in the FQHE regime allows studying a rare example of a non-Fermi electron liquid.

Experimental studies in this field mostly amount to analyzing the tunneling into the edge of a two-dimensional system. Indeed, as was shown for both the IQHE and FQHE regimes [41, 42], the propagation rate of collective excitations is mainly determined by the Hall conductance σ_{xy} and is not very sensitive to the edge structure and the specific features of the collective-mode excitation. The only existing report about observing slow acoustic modes [53] was never confirmed and most probably was a result of registering a usual magnetoplasmon having run around the sample (a so-called round-trip).

On the other hand, collective modes are excited due to tunneling into the edge of the system, and their excitation determines the response of the system to the tunneling into the edge or, in other words, determines the tunnel density of states. Wen [6] has shown theoretically that the tunnel density of states has gapless behavior in the FQHE regime, $D(E) \sim E^{1/g-1}$, which leads to a power-law I–V $I \sim \int D(eV)\,\mathrm{d}V \sim V^{1/g}$, where the universal relation $g = 1/\nu$ holds for the $\nu = 1/3$ filling factor from the principal Laughlin sequence.

From the standpoint of the momentum distribution function of the initial particles (electrons), the non-Fermi behavior is manifested in the disappearance of the Fermi step of the distribution function. The step is replaced by a finite-width area, in which the distribution function smoothly decreases to zero, with the width of the area increasing as the interaction becomes stronger. A finite temperature also causes the 'smearing' of the Fermi step, and hence non-Fermi effects should be exhibited at temperatures lower than some typical one. It was shown in [54] that there are universal scaling relations for the temperature dependence of the tunnel density of states and, correspondingly, of the I–V: $I \sim T^{1/g}$, with the same universal behavior $g = 1/\nu$ for the principal Laughlin sequence. These results have also been confirmed in the approach of composite fermions [55].

In the experimental study of tunneling into the edge, it must be ensured that the I–V nonlinearity is caused precisely by the excitation of collective modes and not by the deformation of the potential barrier. The latter is always the case in the IQHE regime, due to the smoothness of the system edge. In the FQHE regime, where the energy gaps are much smaller (by several orders of magnitude), one can try to realize the case of a sharp edge potential. For this, the so-called cleaved edge overgrowth technique [56] is used. After the growth of a high-mobility two-dimensional system, the side surface of the sample is cleaved right in the camera for molecular-beam epitaxial growth, under a high vacuum. Then the sample is turned, the cleaved edge up, and further growth is made on the cleaved surface. In the simplest version, a tunnel barrier is grown first, and then a strongly doped area for creating a tunnel contact (Fig. 15). Experiments in Refs [56, 57] demonstrated power-law I–Vs in the case of tunneling into the edge, as well as temperature scaling of these diagrams with the exponents close to the predicted ones [6, 54] for the filling factor $\nu = 1/3$. Dependences of the exponents on the filling factor for various experiments and various samples, together with the expected theoretical dependences,

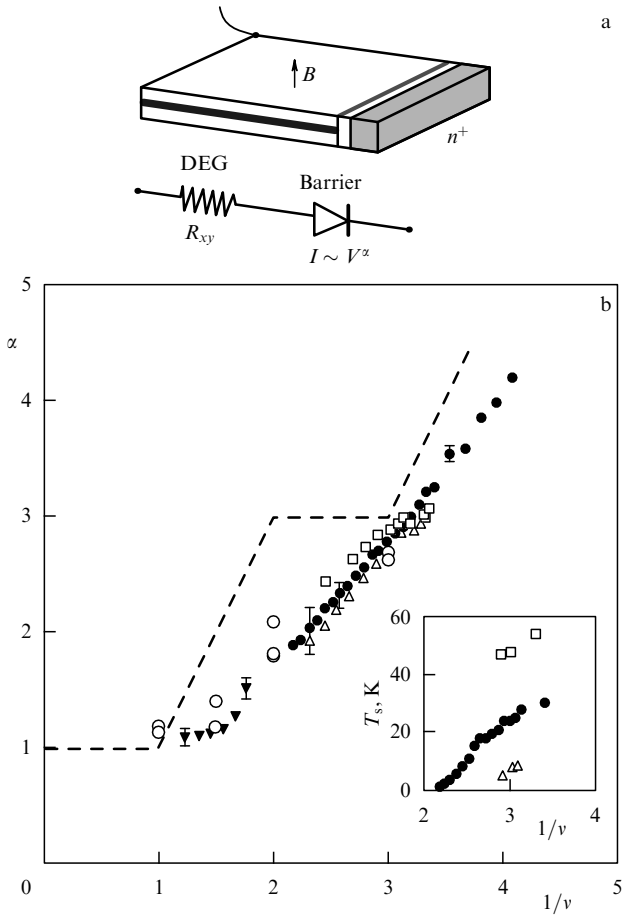

Figure 15. (a) Schematic of the experiment on tunneling into the edge using the cleaved edge overgrowth technique. (b) Exponents of the I–V obtained in experiment (symbols) at different filling factors for various samples obtained by cleaved edge overgrowth, compared with the theoretical dependence (dashed line). (From Ref. [57].)

are shown in Fig. 15. As can be seen from the figure, the experiment and the theory give considerably different results outside the vicinity of $\nu = 1/3$, which, apparently, is caused by a structure of compressible and incompressible strips forming on the edge. This is considered in more detail in Section 3.4.2.

3.3 Edge states: the case of a real potential

An idea that suggests itself is to study edge states in the FQHE regime by means of the crossing gate technique, which turned out to be so helpful in the IQHE regime. However, a difficulty arises here, which has already been mentioned above: the electrostatic potential of a crossing gate cannot be considered rigid even in the FQHE regime. Thus, it is necessary to introduce edge states for a slowly increasing edge potential and to describe their structure.

3.3.1 Structure of a smooth edge and the transport along the edge. For a smooth potential, the bottom of the two-dimensional subband increases in the vicinity of the edge and the electron concentration decreases. Hence, a local filling factor can be introduced, which varies from the bulk value to zero in approaching the edge of the sample. At some points, the local filling factor must take values equal to the fractional filling factors corresponding to the FQHE.

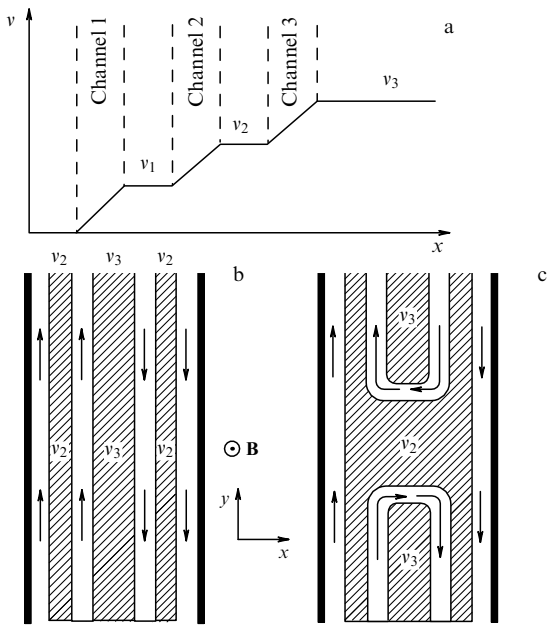

Figure 16. Electron density in the vicinity of the sample edge. (a) The case of a smooth potential. Compressible (white) and incompressible (hatched) areas of the sample: (b) strip of a two-dimensional gas in the quantum Hall effect regime, (c) the same strip crossed by a gate under which there is an incompressible state with the filling factor smaller than the bulk one. (From Ref. [58].)

Beenakker [58] showed that for a sufficiently pure system and the FQHE existing with such local filling factors, finite-width incompressible strips corresponding to these filling factors appear on the edge (Fig. 16). In the FQHE regime, therefore, similarly to the IQHE case [14], a smooth edge consists of alternating strips of compressible and incompressible electron liquid (Fig. 16b).

The difference from the integer case lies in the fact that it is now impossible to introduce a system of Landau levels bent at the edge, because everything occurs on the last (single) Landau level. It can only be asserted that there is no gap in compressible strips, while a gap corresponding to the electrochemical potential between the ground and the excited states occurs in incompressible strips. This gap shrinks at the edges of each incompressible strip. Dissipation-free current, similarly to the IQHE case, is carried by the ground state and, because the 'excess' current is concentrated near the edge of the incompressible area in the absence of equilibrium, it can be described as an edge current.

As in the integer case, the analogue of the Büttiker formalism can now be introduced as [58]

$$I_i = \frac{e}{h}\left(\nu_i \mu_i + \sum_{j \neq i} T_{ij} \mu_j\right), \tag{18}$$

where I_i is the current carried by the edge states coming out of contact i, μ_i is the electrochemical potential of contact i, and ν_i is the maximum filling factor for incompressible strips coming from contact i. It is easy to see that formula (18) contains Büttiker formula (6) as a special case of integer ν_i, as well as MacDonald's result [51] for a sharp edge potential, because $e^* = e\nu$. This is because the Büttiker formalism is a rather general integral relation, which is independent of the details of the edge structure.

Similarly to the integer case, to check the formalism one should place a crossing gate on the sample and in this way restrict the set of possible filling factors to a single one, which is the filling factor of one of the edge strips (Fig. 16b, c). Such experiments showed a perfect agreement between the calculation and the measurement [59].

3.3.2 Edge structure for real edge potentials. Now, the only question remaining is under what conditions a real edge of a system can be considered smooth. The answer was given in several works. Numerical calculations based on the Laughlin wave function [60] and in the framework of the composite-fermion approach [61] showed that the structure of strips of an incompressible and compressible electron liquid already appears at the edge width as small as five or six magnetic lengths. In other words, all real potentials (such as, for instance, the most common potential of a mesa etched edge) satisfy this condition. Even the potential of a cleaved edge cannot be considered sharp, which probably explains the discrepancies between the experimental and calculated exponents in Refs [56, 57].

The composite-fermion approach turns out to be inconvenient for the analysis of the soft edge, because it eventually leads to the same Beenakker – Büttiker relations and the same strip structure of the electron liquid [52, 61] and, moreover, involves serious technical complications. Indeed, for bulk filling factors larger than $1/2$ (for instance, $2/3$) and for the electron density slowly decreasing toward the edge of the sample, there is an area with the local filling factor $1/2$. This area corresponds to a large number of filled Landau levels for composite fermions and, hence, in the vicinity of this area, there should be an infinite number of edge states directed oppositely and nearly compensating each other [52, 61]. So far, there is no experimental evidence in favor of this picture. Hence, the composite-fermion approach, which gives a simple physical picture for the bulk of the sample, leads to a rather complicated and nonphysical picture at a smooth edge.

3.3.3 Collective modes on a smooth edge. As mentioned in Section 3.3.1, strips of incompressible electron liquid exist on a smooth edge of a two-dimensional electron system in the FQHE regime. Edge collective modes appear near the boundaries of these strips [60]. In addition, because the edges of the strips are close (both to each other and to the edges of neighboring strips if the potential is not very smooth), and the electric fields are long-range ones, these modes interact [62]. Therefore, collective excitations on a smooth edge in the FQHE are most similar to neutral magnetoplasmon modes, which were first proposed for the integer effect [43]. As a result, in the case of tunneling into a smooth FQHE edge, the exponent of the tunnel density of states and hence the I – Vs become dependent on the real shape of the edge potential [62], although the I – V maintains its power-law behavior, which seems to have been demonstrated in Refs [56, 57].

3.3.4 Transport across the edge at a small imbalance. Similarly to the IQHE regime, study of the transport across the edge under a small imbalance allows finding the phenomenological equilibration length between edge states. Such experiments have been carried out in the Hall-bar geometry with two crossing barriers (see Fig. 2). It was discovered in Refs [13, 63, 64] that the equilibration length between fractional edge states is of the order of ten micrometers, which is much smaller than in the IQHE regime. This is because at a small imbalance, the equilibration length is mainly determined by the parameters of the tunnel barrier between edge states, which, in turn, depend on the spectral gap. Because the spectral gap is small in the FQHE regime, the equilibration length is also small. This was especially clearly demonstrated in Ref. [13], where dynamic nuclear polarization and its effect on the equilibration between edge states were studied. The Overhauser field, which is caused by dynamic nuclear polarization [12], has an effect on the spin gap separating the edge states [23] and, hence, on the processes of equilibration and on the equilibration length. This leads to a strong hysteresis of the experimental curves.

Incidentally, it is worth mentioning experiments with constrictions (quantum point contacts) [65]. In such experiments, a constriction in the two-dimensional area is created by means of two gates placed close to each other. Due to the structure of the strips of compressible and incompressible electron liquid near each gate and the small separation of the gates, one can study the transport across the edge of such systems. Unfortunately, because the fields of the gates are long-range ones, the bias voltage across the edge deforms the electron density between the gates [66] (in other words, inside the point contact). This transformation of the electron density is the main effect observed in such studies [65].

3.4 Transport across the edge in the strongly nonequilibrium case

As shown in Section 3.3.3, experiments on tunneling into a smooth edge and equilibration on a smooth edge with small imbalance do not allow separating the contribution of collective modes. However, the very smoothness of the edge provides a method to select the contribution of collective modes for strongly nonequilibrium edge states.

The exact shape of the potential barrier separating compressible strips is initially unknown. But in the case of strongly nonequilibrium edge states, this barrier, to a good accuracy, can be considered triangular, while in the limit case, we can definitely assume that the single-electron transmissivity of the barrier is close to unity. Under these conditions, it is impossible to speak about tunneling between edge states, but we can speak of the transport between them, which is then determined only by the effects of collective-mode excitations. In this regime, of considerable interest are not only direct studies of the transport between edge states but also the processes of equilibration at the edge, because they are also determined by collective-mode excitations.

In other words, collective-mode effects can be selected in two limit cases. The first is where the bias potential is so small compared to the potential barrier that it does not deform it. The second case is where the bias potential is too large to deform the barrier. We note that the second case is easier to realize from the experimental standpoint, and it can be better controlled.

3.4.1 Method of study. In the case of imbalance exceeding the spectral gap, the transport was studied in the quasi-Corbino geometry, which allowed creating a strong imbalance and performing direct measurements in this regime (see Section 2.4 about using this geometry in the IQHE regime). Figure 17 shows the structure of compressible and incompressible electron liquid strips near the gate gap of such a

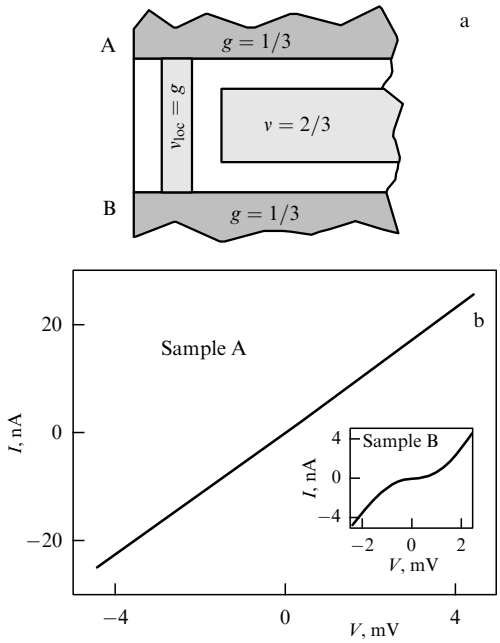

Figure 17. (a) The structure of compressible and incompressible electron liquid strips in the working area of a sample for the filling factors $\nu = 2/3$ and $g = 1/3$ (from Ref. [68]). (b) Examples of linear and strongly nonlinear current – voltage characteristics for samples with different widths of the interaction area and filling factors $\nu = 2/3$ and $g = 1/3$ (from Ref. [20]).

sample for filling factors $g = 1/3$ beneath the gate and $\nu = 2/3$ outside it.

This scheme is based on the data of magnetoresistance and magnetocapacitance measurements. For instance, measuring the magnetoresistance in the quantum Hall effect regime allows finding the field corresponding to the filling factor $\nu = 2/3$ in the part of the sample not covered by the gate. Further, the capacitance between the two-dimensional system and the gate should be measured after a decrease in the electron concentration beneath the gate. This allows finding the FQHE fractional filling factors manifested in the given sample at given magnetic fields due to a decrease in the electron concentration. Because approaching the edge is also accompanied by a decrease in the electron concentration (see Section 3.3), we can be sure that incompressible strips appear at the edge of the sample at the same filling factors that were observed when decreasing the electron density beneath the gate. Indeed, in the sample described in Ref. [20], with the bulk filling factor $\nu = 1$, incompressible strips appear in the vicinity of the edge with local filling factors 2/3 and 1/3. Choosing the filling factor beneath the gate to coincide with one of these values, we choose the incompressible strip for which the transport is studied.

Similarly to the IQHE case, obtaining current – voltage characteristics is the basic tool in the study of the transport. Measurement of the transport through an incompressible strip can be carried out in two ways: by fixing the current or by fixing the voltage. Because the FQHE is especially sensitive to the quality of the samples and manufacturing ohmic contacts for such samples is extremely difficult, to check the results for reliability it is necessary to see whether the data of both above-described methods of the I – V measurement agree in each particular case. In addition, it is necessary to independently estimate the resistance and the quality of the contacts using magnetoresistance measurements, to use various samples and different methods to cool them, and to compare the results with the ones known for the IQHE regime.

Similarly to the IQHE regime, changing the length of the interaction area with respect to the edge-state equilibration length (which depends on the temperature and on the magnetic field), allows studying the transport either in the regime of complete equilibration (linear I – Vs) or in the strongly nonequilibrium regime (strongly nonlinear I – Vs). Examples of both linear and nonlinear I – Vs for the filling factors $\nu = 2/3$, $g = 1/3$ are shown in Fig. 17.

3.4.2 Equilibration at the edge and the structure of edge states. Direct measurements of the *structure* of edge collective excitations (in the cases where the structure is assumed to be complicated) are not realistic: they would require an independent study of several simultaneously propagating magnetoplasmon modes [42]. But an indirect measurement method is possible. During the equilibration from an initially strongly nonequilibrium case, the transport across an incompressible strip involves excitation of the same collective modes, which, in turn, establish the edge potential and therefore influence the equilibration [67]. Such effects are not taken into account by the single-particle Büttiker – Beenakker theory. Hence, from the comparison between the experimental equilibrium resistance and the one calculated according to Büttiker's formalism, one can learn about collective excitations at the edge.

To compare the structure of edge states with the expected one, equilibration at the edge was studied in Ref. [20]. For this, the transport was studied through incompressible strips corresponding to the local filling factors $\nu_{loc} = g = 2/3, 1/3$, the bulk filling factor being $\nu = 1$. This method of study allows investigating equilibration with a fixed strip structure and with a fixed disorder in the interaction area, i.e., under fixed conditions, by varying only the electron concentration beneath the gate, i.e., by realizing contacts between different compressible strips. Büttiker's calculation (see Sections 2.4.2 and 3.3.1) yields the same equilibrium values of resistance for both combinations of filling factors. However, the experiment in [20] showed the equilibrium resistance values to be different: for the transport through the incompressible strip with the local filling factor 2/3, the slope of the equilibrium curve turned out to be much *smaller* than the expected one, while for the transport through the strip with the filling factor 1/3, the measured slope was close to the expected one. The difference in the slopes of the equilibrium curves decreases when a tangential magnetic field is applied to the sample.

The difference in the slopes discovered in Ref. [20] cannot be explained by the difference in the resistance of the contacts because the measured resistances are *smaller* than the equilibrium ones. In terms of Büttiker's formalism, this corresponds to an *excess* charge transfer between the edge states, which is difficult to explain in the framework of this formalism. At the same time, the filling factor 2/3 is distinguished in this experiment only by the fact that for the edges of the strip 2/3, a complicated structure of collective modes is expected [6, 51], and interaction between these modes determines the 'excess' equilibration of edge states. Thus, the experiment in Ref. [20] for the first time demonstrated the existence of several branches of collective excitations at the edge of an FQHE system with the filling factor 2/3.

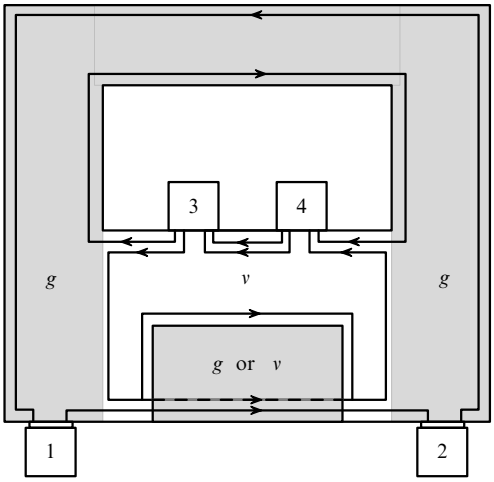

Figure 18. Schematic of a sample for the study of relaxation to equilibrium at the edge for large length scales. (From Ref. [19].)

3.4.3 Equilibration for large length scales. In Ref. [19], the influence of collective modes on the equilibration at the edge was studied under the variation of the gate gap (the interaction area). The study was aimed at transforming a strongly nonlinear current – voltage characteristic into a linear one (see Fig. 17) without changing the state of the two-dimensional electron system in the sample. For this, the structure of the sample in the quasi-Corbino geometry was modified (Fig. 18).

The gap area in the outer-edge gate was made macroscopically large, about 800 μm. In this area, an additional gate was placed, separated from the main one by 5 mm-wide slits. This way, measurements could be carried out in two regimes:

(1) the additional gate is grounded and the electron concentration beneath it is the same as outside the gate. Then the interaction area of edge states has the width 800 μm;

(2) the additional gate has the same potential as the main one and separates edge states: one of them is beneath the gate and the other one is at its edge. (The gate width is 200 μm, which is sufficient for the full cancellation of transport between edge states.) There are two edge-state interaction areas, each having the width 5 μm, separated by a macroscopic distance and therefore independent. The full width of the interaction area is in this case 10 μm.

Thus, varying the voltage at the additional gate allows controlling the width of the interaction area.

Transformation of current – voltage characteristics for the filling factors $\nu = 2/3$, $g = 1/3$ due to the change in the interaction area size from 10 to 800 μm is shown in Fig. 19. As expected, the diagrams for these factors, initially weakly nonlinear, turn into linear ones with the slope coinciding with the one found from the Büttiker – Beenakker calculation. The linearity of the central part of the curves means that the equilibration length does not exceed the interaction area size at small imbalances. Based on these considerations, the equilibration length can be estimated to be 10 μm, which is in agreement with the results in Refs [63, 64] obtained at small imbalances.

The most unexpected result is the transformation of I – Vs corresponding to the filling factors $\nu = 2/5$, $g = 1/3$ (see Fig. 19). From the weakly nonlinear I – V, which is higher than the calculated equilibrium dependence, the equilibration length for edge states can be estimated to exceed 10 μm. As the interaction area increases, the I – V remains weakly nonlinear (see the inset in Fig. 19b) but lies *below* the equilibrium calculated curve, which would correspond, in terms of the Beenakker – Büttiker single-particle picture, to *excessive* charge transfer (by more than a quarter). Nonlinear curves for both lengths of the interaction area can be reduced to a single curve by expanding (or compressing) them along the current axis. In this case, the scaling coefficient is 40 times less than the ratio of the interaction area lengths.

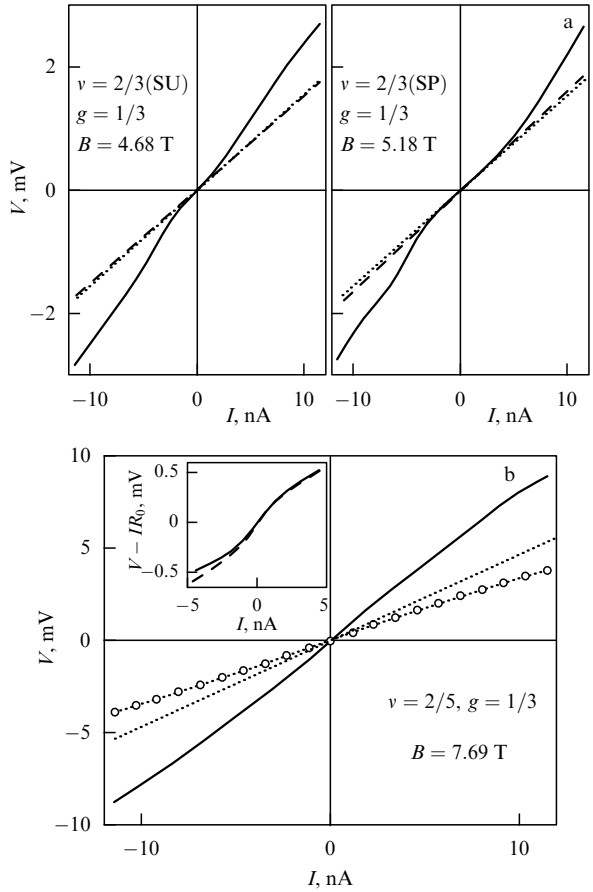

Figure 19. (a) Transformation of the I – V due to the increase in the interaction area for the filling factors $\nu = 2/3$, $g = 1/3$ and for two spin polarizations of the $\nu = 2/3$ state: SP (spin-polarized) and SU (spin-unpolarized). (b) Transformation of the I – V due to the increase in the interaction area for the filling factors $\nu = 2/5$, $g = 1/3$. Solid lines correspond to the small length of the interaction area, dashed lines to the macroscopic length of the interaction area, and dotted lines to the equilibrium theoretical dependences. The dotted line marked with circles is the main experimental result. The inset shows the scaling of current – voltage characteristics obtained for various lengths of the interaction area. Nonlinearity of I – Vs is demonstrated. (From Ref. [19].)

We note that prior to Ref. [19], no edge-state experiments have been carried out for filling factors other than 2/3 and 1/3. What is so special and interesting about the filling factor 2/5? We consider the structure of compressible and incompressible strips in the interaction area in more detail (see Fig. 17).

The strip structures for filling factors $\nu = 2/3$, $g = 1/3$ and $\nu = 2/5$, $g = 1/3$ are qualitatively similar. Moreover, the transport occurs through the same incompressible strip, corresponding to the local filling factor 1/3. But the width

of the compressible strip separating this incompressible strip from the rest of the sample is different in these two cases. If the edge potential is the same, this width is determined by the difference in the local filling factors: $2/3 - 1/3 = 1/3$ and $2/5 - 1/3 = 1/15$. Thus, the bulk filling factor $2/5$ is very close to the transport incompressible strip. In this particular case, collective modes are therefore excited not only at the boundaries of the strip with the filling factor $1/3$ but also at the boundary of the bulk filling factor $2/5$. In other words, this case corresponds to the excitation of the soft magnetoplasmon mode [43]. In addition, because of the special features of the collective modes on the $2/5$ boundary, they are expected to have a considerable impact on the equilibration [67].

3.4.4 Transport through a incompressible strip in the case of large imbalance. The study of equilibration in Refs [20, 19] experimentally demonstrated the impact of soft collective modes on the transport through an incompressible strip, but these results can hardly be used for a quantitative analysis of such modes. More appropriate is the study of transport at small lengths, which in fact means point-like excitation of collective modes.

We consider a current carried across an incompressible strip, shown in Fig. 17a, depending on the equilibration length:

$$I = R_{\mathrm{eq}}^{-1} V \left[1 - \exp\left(-\frac{L_{\mathrm{AB}}}{l_{\mathrm{eq}}} \right) \right] . \tag{19}$$

For $L_{\mathrm{AB}} \ll l_{\mathrm{eq}}$, the shape of the current – voltage characteristic directly reflects the behavior of the equilibration length as the imbalance between the edge states is varied. In turn, the equilibration length reflects the behavior of the transition probability between the edge states, $l_{\mathrm{eq}} \sim w^{-1}$. The transition probability can be written as the single-particle transmissivity of the potential barrier times the tunnel density of states: $w \sim T_0(V) D(V, T)$. As mentioned in Section 3.4, the barrier can be considered triangular in the strongly nonequilibrium case, and therefore the single-particle transmittance, which can be written as $\exp(-C\Delta^{3/2}/V)$, tends to unity when the imbalance exceeds the fractional gap.

Because the equilibration length for fractional filling factors and small imbalances was known to be of the order of 10 μm, the samples used in Ref. [68] had the width of their working area equal to 0.5 μm.

Figure 20a shows examples of I – Vs for integer and fractional filling factors in samples with small working areas. The differences in the I – Vs for fractional filling factors from the well-known I – Vs for integer filling factors are (1) the absence of a threshold; (2) strong nonlinearity within the whole voltage range; and (3) almost perfect symmetry. This behavior of the I – Vs is observed for almost all fractional filling factors.

Equilibration lengths calculated by means of formula (19) for various filling factors are shown in Fig. 20b. For integer filling factors, the l_{eq} behavior corresponds to the known one caused by the deformation of the potential barrier between edge states, while for fractional filling factors, the behavior of l_{eq} was studied in Ref. [68] for the first time.

Under these conditions, the transition probability dependence on imbalance and temperature reflects the dependence of the tunnel density of states on these parameters. The tunnel

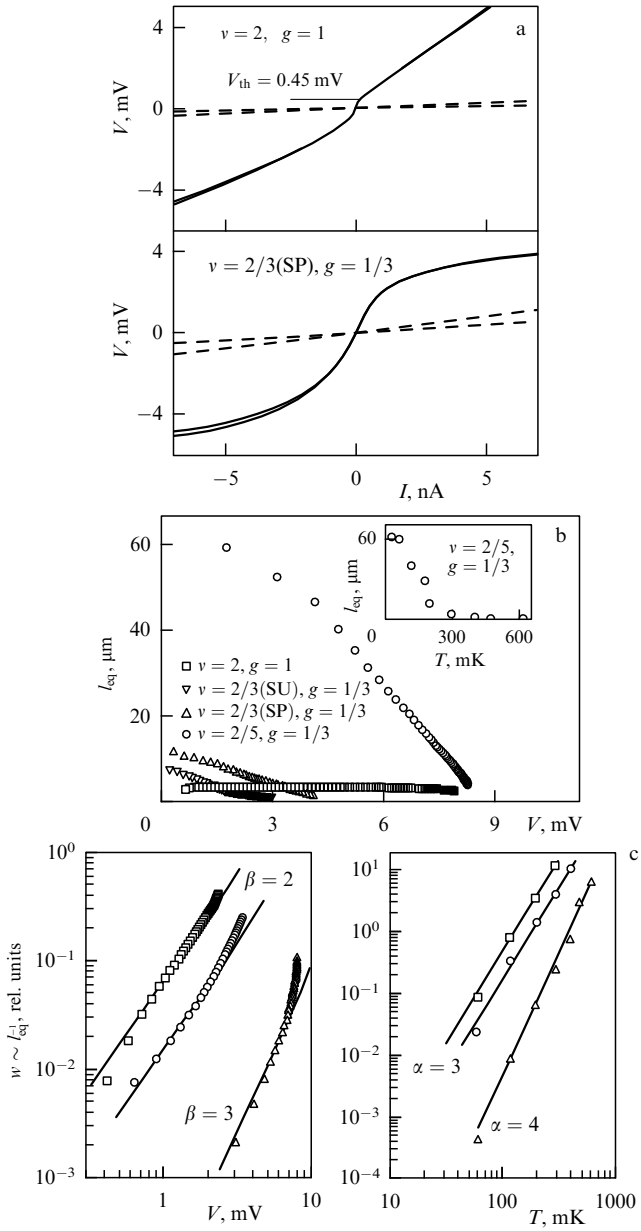

Figure 20. (a) Examples of current – voltage characteristics for integer and fractional filling factors in samples with a small width of the working area (0.5 μm). Solid lines correspond to experimental data, dashed lines show the equilibrium theoretical dependences. (b) Equilibration length for various filling factors depending on the value of imbalance. (c) Power-law behavior of the transition probability at a smooth edge as a function of the imbalance and temperature. (From Ref. [68].)

density of states, due to the collective-mode effects, has power-law dependences on the temperature and imbalance. The power-law behavior of the transition probability was demonstrated in Ref. [68] (Fig. 20c); the exponents found in experiment for the voltage and temperature dependences differ by unity, as indeed should be the case under the excitation of collective modes [6, 54]. The exponents were found in Ref. [68] for the first time and need a theoretical explanation. They are different for the filling factors $\nu = 2/3$, $g = 1/3$ and $\nu = 2/5$, $g = 1/3$, which is caused by the collective-mode excitation at the boundary of the bulk filling factor $\nu = 2/5$, i.e., by the excitation of the soft magnetoplasmon mode.

3.5 Main conclusions for the fractional quantum Hall effect

We summarize the results of studying edge states in the FQHE regime.

• Fundamental results in explaining the FQHE were obtained by means of the Laughlin theory.

• The composite-fermion hypothesis, although being simple and nice, has so far not been completely confirmed and requires additional studies, both theoretical and experimental.

• Under the conditions of the fractional quantum Hall effect, the edge of the system consists of alternating strips of compressible and incompressible electron liquid.

• The propagation rate of collective excitations along the edge of the sample is mainly determined by Hall's conductance and, as in the case of the IQHE, has little sensitivity to the edge structure.

• For edge states, the influence of the tunnel density of states, which depends on collective effects, is most pronounced in two limit cases: for an infinitely high barrier, which is not deformed by a bias potential, and for an infinitely narrow barrier, which is completely transparent for single-particle tunneling.

• The tunnel density of states has an impact on all effects related to the transport between edge states, both in the direct studies of the transport and in the studies of equilibration between edge states.

4. Conclusion

We outline the problems that are important for further progress in the considered field of physics.

Graphene. Recently, two-dimensional structures have been created based on graphene, thin films of graphite coated on the surfaces of silicon oxide [69]. The quantum Hall effect has already been observed in such structures, which provide high mobility. There is special interest in graphene because of the assumption that the spectrum of carriers in a two-dimensional subband is linear, which should have an effect on many physical properties. The study of edge states in graphene is a completely new and unexplored field.

Edge reconstruction. The question about the effect of the electron – electron interaction on the structure of edge states is from time to time discussed in theoretical publications. Indeed, Refs [70] predicted that a complicated rearrangement of the electron density should occur on the edge (the edge reconstruction): there should be a local maximum at the very edge, then the density should drop dramatically almost to zero, and then it should increase up to its bulk value. Such a structure has never been observed in experiment. It is possible, however, that it can be created artificially, similarly to the way topological defects were created. Another open question is about the edge reconstruction in graphene samples.

Acknowledgements

The author is grateful to V T Dolgopolov for fruitful discussions during the preparation of this review and to D E Feldman for valuable remarks that helped in understanding many theoretical works. The work was supported by the RFBR, programs of RAS, the Program of State Support of Leading Scientific Schools, the Foundation for Promotion of Russian Science, and the President's Grant of Young Scientists Support MK-4232.2006.2.

References

1. Khaikin M S *Pis'ma Zh. Eksp. Teor. Fiz.* **4** 164 (1966) [*JETP Lett.* **4** 113 (1966)]; *Zh. Eksp. Teor. Fiz.* **55** 1696 (1968) [*Sov. Phys. JETP* **28** 892 (1969)]
2. Prange R E, Girvin S M (Eds) *The Quantum Hall Effect* (New York: Springer-Verlag, 1987) [Translated into Russian (Moscow: Mir, 1989)]
3. Landauer R *Philos. Mag.* **21** 863 (1970)
4. Büttiker M *Phys. Rev. B* **38** 9375 (1988)
5. Luttinger J M *J. Math. Phys.* **4** 1154 (1963)
6. Wen X-G *Phys. Rev. B* **43** 11025 (1991); *Phys. Rev. Lett.* **64** 2206 (1990); *Phys. Rev. B* **44** 5708 (1991)
7. Haug R J *Semicond. Sci. Technol.* **8** 131 (1993)
8. Landau L D, Lifshitz E M *Kvantovaya Mekhanika*: *Nerelyativistskaya Teoriya* (Quantum Mechanics: Non-Relativistic Theory) (Moscow: Fizmatlit, 2001) [Translated into English (Oxford: Pergamon Press, 1977)]
9. Halperin B I *Phys. Rev. B* **25** 2185 (1982)
10. Müller G et al. *Phys. Rev. B* **45** 3932 (1992)
11. Khaetskii A V *Phys. Rev. B* **45** 13777 (1992)
12. Dixon D C et al. *Phys. Rev. B* **56** 4743 (1997)
13. Machida T et al. *Phys. Rev. B* **65** 233304 (2002)
14. Chklovskii D B, Shklovskii B I, Glazman L I *Phys. Rev. B* **46** 4026 (1992)
15. Ahlswede E et al. *Physica E* **12** 165 (2002)
16. Thouless D J *Phys. Rev. Lett.* **71** 1879 (1993)
17. Müller G et al. *Surf. Sci.* **263** 280 (1992)
18. Würtz A et al. *Phys. Rev. B* **65** 075303 (2002)
19. Deviatov E V et al. *Phys. Rev. B* **74** 073303 (2006)
20. Deviatov E V et al. *Pis'ma Zh. Eksp. Teor. Fiz.* **82** 598 (2005) [*JETP Lett.* **82** 539 (2005)]
21. Dolgopolov V T et al. *Phys. Rev. Lett.* **79** 729 (1997)
22. Deviatov E V, Dolgopolov V T, Würtz A *Pis'ma Zh. Eksp. Teor. Fiz.* **79** 618 (2004) [*JETP Lett.* **79** 504 (2004)]
23. Deviatov E V et al. *Phys. Rev. B* **69** 115330 (2004)
24. Davies A G et al. *Phys. Rev. B* **54** R17331 (1996)
25. Dolgopolov V T et al. *Phys. Rev. B* **59** 13235 (1999)
26. Deviatov E V et al. *Pis'ma Zh. Eksp. Teor. Fiz.* **71** 724 (2000) [*JETP Lett.* **71** 496 (2000)]
27. Sawada A et al. *Phys. Rev. Lett.* **80** 4534 (1998); *Phys. Rev. B* **59** 14888 (1999)
28. Pellegrini V et al. *Phys. Rev. Lett.* **78** 310 (1997); *Science* **281** 799 (1998)
29. Khrapai V S et al. *Phys. Rev. Lett.* **84** 725 (2000)
30. Das Sarma S, Sachdev S, Zheng L *Phys. Rev. Lett.* **79** 917 (1997); *Phys. Rev. B* **58** 4672 (1998); Demler E, Das Sarma S *Phys. Rev. Lett.* **82** 3895 (1999); Brey L, Demler E, Das Sarma S *Phys. Rev. Lett.* **83** 168 (1999)
31. Jungwirth T et al. *Phys. Rev. Lett.* **81** 2328 (1998); MacDonald A H, Platzman P M, Boebinger G S *Phys. Rev. Lett.* **65** 775 (1990)
32. Iordanski S V, Kashuba A *Pis'ma Zh. Eksp. Teor. Fiz.* **75** 419 (2002) [*JETP Lett.* **75** 348 (2002)]
33. Deviatov E V et al. *Pis'ma Zh. Eksp. Teor. Fiz.* **79** 206 (2004) [*JETP Lett.* **79** 171 (2004)]
34. Dempsey J, Gelfand B Y, Halperin B I *Phys. Rev. Lett.* **70** 3639 (1993); Gelfand B Y, Halperin B I *Phys. Rev. B* **49** 1862 (1994)
35. Rijkels L, Bauer G E W *Phys. Rev. B* **50** 8629 (1994)
36. Deviatov E V et al. *Phys. Rev. B* **72** 041305(R) (2005)
37. Deviatov E V et al. *Pis'ma Zh. Eksp. Teor. Fiz.* **75** 36 (2002) [*JETP Lett.* **75** 34 (2002)]
38. Volkov V A, Mikhailov S A *Zh. Eksp. Teor. Fiz.* **94** 217 (1988) [*Sov. Phys. JETP* **67** 1639 (1988)]
39. Wassermeier M et al. *Phys. Rev. B* **41** 10287 (1990); Grodnensky I, Heitmann D, von Klitzing K *Phys. Rev. Lett.* **67** 1019 (1991); Talyanskii V I et al. *Phys. Rev. B* **46** 12427 (1992)
40. Ashoori R C et al. *Phys. Rev. B* **45** 3894 (1992); Zhitenev N B *Pis'ma Zh. Eksp. Teor. Fiz.* **55** 722 (1992) [*JETP Lett.* **55** 756 (1992)]
41. Zhitenev N B et al. *Phys. Rev. Lett.* **71** 2292 (1993)
42. Ernst G et al. *Phys. Rev. Lett.* **79** 3748 (1997)
43. Aleiner I L, Glazman L I *Phys. Rev. Lett.* **72** 2935 (1994)
44. Deviatov E V et al. *Appl. Phys. Lett.* **71** 3655 (1997)
45. Laughlin R B *Phys. Rev. Lett.* **50** 1395 (1983)

46. Halperin B I *Helv. Phys. Acta* **56** 75 (1983); Xie X C, Guo Y, Zhang F C *Phys. Rev. B* **40** 3487 (1989); Chakraborty T, Pietiläinen P *Phys. Rev. B* **41** 10862 (1990)
47. Eisenstein J P et al. *Phys. Rev. B* **41** 7910 (1990); Engel L W et al. *Phys. Rev. B* **45** 3418 (1992); Kang W et al. *Phys. Rev. B* **56** R12776 (1997)
48. Dolgopolov V T et al., cond-mat/0606716; *Phys. Status Solidi B* **243** 3648 (2006)
49. Jain J K *Phys. Rev. Lett.* **63** 199 (1989)
50. Willett R L et al. *Phys. Rev. Lett.* **71** 3846 (1993)
51. MacDonald A H *Phys. Rev. Lett.* **64** 220 (1990)
52. Brey L *Phys. Rev. B* **50** 11861 (1994)
53. Ernst G et al. *Phys. Rev. Lett.* **77** 4245 (1996)
54. Kane C L, Fisher M P A *Phys. Rev. B* **46** 15233 (1992); *Phys. Rev. Lett.* **68** 1220 (1992)
55. Shytov A V, Levitov L S, Halperin B I *Phys. Rev. Lett.* **80** 141 (1998)
56. Chang A M, Pfeiffer L N, West K W *Phys. Rev. Lett.* **77** 2538 (1996)
57. Grayson M et al. *Phys. Rev. Lett.* **80** 1062 (1998); Hilke M et al. *Phys. Rev. Lett.* **87** 186806 (2001)
58. Beenakker C W J *Phys. Rev. Lett.* **64** 216 (1990)
59. Syphers D A, Stiles P J *Phys. Rev. B* **32** 6620 (1985); Haug R J et al. *Phys. Rev. Lett.* **61** 2797 (1988); Washburn S et al. *Phys. Rev. Lett.* **61** 2801 (1988); Matsuda Y et al. *Phys. Rev. B* **40** 5176 (1989)
60. Chamon C de C, Wen X G *Phys. Rev. B* **49** 8227 (1994)
61. Chklovskii D B *Phys. Rev. B* **51** 9895 (1995)
62. Conti S, Vignale G *Phys. Rev. B* **54** R14309 (1996)
63. Kouwenhoven L P et al. *Phys. Rev. Lett.* **64** 685 (1990)
64. Chang A M, Cunningham J E *Phys. Rev. Lett.* **69** 2114 (1992)
65. Roddaro S et al. *Phys. Rev. Lett.* **93** 046801 (2004); **95** 156804 (2005)
66. Shashkin A A et al. *Pis'ma Zh. Eksp. Teor. Fiz.* **69** 561 (1999) [*JETP Lett.* **69** 603 (1999)]
67. Zülicke U, Shimshoni E *Phys. Rev. B* **69** 085307 (2004); *Phys. Rev. Lett.* **90** 026802 (2003)
68. Deviatov E V et al., cond-mat/0606741
69. Novoselov K S et al. *Nature* **438** 197 (2005)
70. Wan X, Yang K, Rezayi E H *Phys. Rev. Lett.* **88** 056802 (2002); Wan X, Rezayi E H, Yang K *Phys. Rev. B* **68** 125307 (2003)